Universitat Politècnica de Catalunya
Facultat de Matemàtiques i Estadística

Degree in Mathematics

Bachelor's Degree Thesis

Simulation of Massless Oscillations in Biological Tissues with Delayed Differential Equations

Elena Moral Sánchez

Supervised by Jose Javier Muñoz Romero

June, 2019

I would like to give special credit to my supervisor Jose Javier Muñoz Romero for all the dedication to share his knowledge with me, the numerous hours assisting me in solving doubts and answering my questions and his will to make this project advance.

I would like to thank professor Johannes Müller, from TU Munich, for introducing me into the fascinating world of mathematics in bioscience and inspiring me to follow this academic path. I would also like to thank Weibo Li, Oleg Tischenko and all my former colleagues from the Intitute for Radiation Protection at Helmholtz Zentrum München for giving me the chance to have my first experience in professional biomedical research and making my stay fruitful and enjoyable.

I would like to thank my friend David Doste for his assistance and help trying to solve the doubts I encountered throughout this project.

I would like to thank my friends for giving me the encouragement to continue further.

I would like to thank Guillaume, for his limitless love and inspiration to overcome difficulties.

Lastly, I would like to thank my family for the unconditional support during my studies.

Abstract

Oscillations in biological tissues have been observed in multiple processes: gene regulatory signaling, cardiac pulsation, shear waves in cardiac tissue, chemical synapses in neural loops or pattern formation during embryo segmentation [2]. In this project we will focus on displacement oscillations, which appear in tissue deformation processes. These oscillations are a consequence of the forces generated by the cells under stress and they can result in the creation of new tissue structures. They can be classified in three different regimes: stable non-oscillatory, stable oscillatory and unstable.

In this project, we focus on displacement oscillations observed in embryonic tissues and make an attempt to model them through a cell delayed visco-elastic response following the model in [2]. This will require the use of delayed differential equations and the assumption of mechanical equilibrium. Two different models are studied analytically in order to determine the stability. A numerical analysis will also be performed to corroborate the analytic results. The visible oscillations are obtained only when multiple delays coexist.

Keywords

Oscillations, Delay Differential Equations, Delay, size-dependent Delay, DDE, multiple delay, Biological Tissues, Stability, Dynamical Systems

Contents

1 Introduction **3**

1.1 Cell Model . . . 3

1.2 Stability in Ordinary Differential Equations (ODE) . . . 5

1.3 A brief introduction to Delay Differential Equations (DDE) . . . 6

2 Methodology **12**

2.1 First Model . . . 12

2.1.1 Linear Analysis . . . 16

2.1.2 Numerical Analysis . . . 24

2.2 Second Model . . . 29

2.2.1 Linear Analysis . . . 33

2.2.2 Numerical Analysis . . . 40

3 Conclusions **46**

3.1 Future Work . . . 47

4 Bibliography **49**

A Developments and Computations **50**

A.1 First Model Linearisation . . . 50

A.2 Second Model Linearisation . . . 52

B Codes **53**

B.1 Non Linear System First Model . . . 53

B.2 Non Linear System First Model with I_i- dependant delays . . . 54

B.3 CheckStable . . . 56

1. Introduction

Tissue deformation plays a very important role in many different biological processes. For instance, the contraction of epithelial tissue is key in the process of wound healing. It has been observed that during biological tissue deformation, cells generate forces to stretch or shrink their surface, making possible the generation of curved tissues and a variety of new complex tissue structures. With the purpose of giving a context for the mathematical nature of this project, in the following paragraphs some examples of biological tissue deformation are given, accompanied by the respective source article and a brief summary.

Wound healing is an example of epithelial cells movement. Force patterns have been observed during wound closure, which have strong force components that are both radial and tangential to the wound [7]. It has also been shown that these force components are generated by the tensions transmitted by the assembly of a supracellular actomyosin ring surrounding the wound. The bordering cells progressively elongate their shape in order to cover a larger wounded area, while remaining tightly connected to their neighbours through adherens junctions and tight junctions [7].

Dorsal closure is a process which occurs during *Drosophila* embryogenesis and consists on the closing of an epidermal opening. Initially, a supracellular actin cable surrounding the opening appears and provides a contractile force. Amnioserosa cells that fill the opening produce an additional critical force pulling on the surrounding epidermal tissue and leading to displacement. It has been shown that this force is pulsed and is controlled by tension and cell coupling [5]. Also in [5], adjacent visco-elastic polygons were used to represent each cell and its neighbours. Besides, a time delay was introduced in order to resemble the reaction time before contraction initiation, which is essential for further sustained oscillation. It has also been shown that during amnioserosa contraction, the shrinkage of apical cell area is coordinated with the adherens junction length reduction, mantaining a contant junctional straightness, i.e. the global tissue geometry [4].

In [2], displacement oscillations observed in embryonic tissues are modelled through a delayed response. The deformation results from a stress field induced by the displacement. Furthermore, the necessity to include the delay is based on empirical evidence. For example, in the case of chemical signalling, the delay can be justified by the distance the signal has to go through or the time the signal processing may take. The introduction of this delay implies a much more complex stability behaviour and the need to model these oscillations through delay differential equations.

In this project, we introduce two biophysical models based on delay differential equations, analogous to the model studied in [2] through visco-elastic rheological laws and the assumption of mechanical equilibrium. Each model is translated into a system of equations which is analytically and numerically studied in an attempt to determine and corroborate its stability.

1.1 Cell Model

The model we resort to is based on [2] and resembles a viscoelastic delayed response to displacement of each cell wall. The reason behind this is the empirical observation and the evidence of delay given above. We will also impose mechanical equilibrium in order to avoid underdetermined systems.

From this point on, we will often use the term 'edges' to refer to the cell walls. This is due to the simplification of modelling cell walls as line elements. For simplicity purposes, throughout this project some global assumptions are made:

1. In rest position -under no displacement-, all the cells are identical.
2. In rest position, cells are square-shaped. Every cell is represented by the area enclosed by four edges.
3. The cell height remains constant along time.

Consider a cell wall as an isolated line element and assume a displacement is acting on it.

Definition 1.1. The **deformed length** of an edge, represented by $l(t)$ is the visible apparent length.

Definition 1.2. The **rest-length** of an edge, represented by $L(t)$ is the length of the wall at instant t in the stress free configuration. It is an internal variable which does not necessarily correspond to the measurable length of the edge, i.e. in general $l(t) \neq L(t)$.

Remark 1.3. Notice how in elastic springs, the rest-length would be constant, thus 'under absence of forces the spring always returns to its rest position'. However, here we are modelling cell walls' response to displacement with a viscoelastic rheological law. We will dig more into detail later on.

Definition 1.4. The **stress force** acting upon the edge is denoted by $\sigma(t)$ and modelled by the following law [28]:

$$\sigma(t) = k(l(t) - L(t)) \tag{1}$$

Where $l(t) - L(t)$ is a displacement based strain measure and the constant $k > 0$ is a measure of stiffness. We will consider that all the cell walls have the same stiffness.

Remark 1.5. Notice again that for $L(t)$ constant, this equation becomes Hooke's Law for elastic springs.

Definition 1.6. The time evolution equation for the rest-length is given by the following delayed differential equation [28]:

$$\begin{cases} \dot{L}(t) = \gamma(l(t-\tau) - L(t-\tau)) \\ L(t) = L_0, \quad \forall t \leq 0 \end{cases} \tag{2}$$

Where:

The **remodelling rate**, denoted by γ, is a strictly positive real constant and we will consider it to be the same for all the cells.

The **delay of the response** is denoted by τ and it is a positive real constant.

Remark 1.7. We can finally interpret the 'capacity to adapt' of the cell wall:

(i) An expanded edge, i.e. $l(t) > L(t)$, implies that after a period of time τ, the rest-length will increase.

(ii) A contracted edge, i.e. $l(t) < L(t)$, implies that after a period of time τ, the rest-length will decrease.

This can be interpreted as the cells change their rest-shape in order to adapt to their deformed state in the past.

Moreover, a contracted edge corresponds to an outwards stress force, while an expanded edge corresponds to an inwards stress force.

Lastly, consider the case where n cell walls interact with each other through stress forces due to a displacement. We will introduce the concept of mechanical equilibrium in order to impose it on the system.

Definition 1.8. The **elastic energy** of the system at instant t is given by the function:

$$W(t) = \sum_{1 \leq i \leq n} \frac{1}{2} k (l_i(t) - L_i(t))^2 \tag{3}$$

The **equilibrium condition** corresponds to minimizing the energy of the system:

$$\delta W \Big|_{L_i = L_{0,i}} = 0 \Rightarrow \frac{\partial W}{\partial u} \delta u = 0 \quad \forall \delta u \Rightarrow \frac{\partial W}{\partial u} \Big|_{L_i = L_{0,i}} = 0 \Rightarrow \sum_{1 \leq i \leq n} \frac{\partial W}{\partial l_i} \frac{\partial l_i}{\partial u} = 0 \Rightarrow \sum_{1 \leq i \leq n} \sigma_i(t) \frac{\partial l_i}{\partial u} = 0$$

Equilibrium is reached when the sum of the components of stress forces is zero.

Our model requires an introduction to Delay Differential Equations, which will start by a small review of Ordinary Differential Equations and stability.

1.2 Stability in Ordinary Differential Equations (ODE)

An Ordinary Differential Equation of **order** n has the following expression:

$$x^{(n)} = F(t, x, x', ..., x^{(n-1)})$$

where $x^{(k)} := \dfrac{d^{(k)}x}{dt^{(k)}}$, $x(t) \in \mathbb{R}$ and $F \in \mathcal{C}(\mathbb{R}^n, \mathbb{R})$.

It can be reduced to a first-order system by defining the variables $x_i = x^{(i-1)} \quad \forall i$.

$$\begin{cases} x_1' = x_2 \\ \vdots \\ x_{n-1}' = x_n \\ x_n' = F(t, x_1, ..., x_n) \end{cases}$$

The system becomes first-order and n-dimensional:

$$\dot{\mathbf{z}}(t) = \widetilde{\mathbf{F}}(t, \mathbf{z})$$

Where $\mathbf{z}(t) = (x_1, ..., x_n)$ and $\widetilde{\mathbf{F}}(t, \mathbf{z}) = (x_2, ..., x_n, F(t, x_1, ..., x_n))$.

Observe that if $\widetilde{\mathbf{F}}$ is not a linear function, we can linearize it at a point, usually the initial condition given by the ODE.

A **first-order linear ODE** has the following expression:

$$\dot{x}(t) = Ax(t) + b$$

Where A is the system matrix.

Proposition 1.9. *The stability of the first-order linear ODE system $\dot{x}(t) = Ax(t) + b$ is classified as:*

If $\rho(A) \subset \mathbb{R}_{\leq 0}$, the system is **non-oscillatory stable**.

If $\rho(A) \subset \{z \in \mathbb{C} | Re(z) \leq 0\}$ and $\rho(A) \nsubseteq \mathbb{R}_{\leq 0}$, the system is **oscillatory stable**.

If $\rho(A) \cap \{x \in \mathbb{C} | Re(z) > 0\} \neq \varnothing$, the system is **unstable**.

Where $\rho(A)$ is the spectrum of matrix A.

1.3 A brief introduction to Delay Differential Equations (DDE)

The general form of a first order Delay Differential Equation is given by:

$$\dot{\mathbf{x}}(t) = \mathbf{f}(t, \mathbf{x}(t), \mathbf{x_t})$$

Where $\mathbf{x}(t) \in \mathbb{R}^n$ and $\mathbf{x_t} = \{\mathbf{x}(\tau) : \tau \leq 0\}$ is the delayed solution.

In this project, we will work with discrete delays and linear DDEs.

A **linear delay differential equations system with discrete delays** can be expressed as:

$$\dot{\mathbf{x}}(t) = \mathbf{A_0}\mathbf{x}(t) + \mathbf{A_1}\mathbf{x}(t-\tau_1) + \mathbf{A_2}\mathbf{x}(t-\tau_2)) + ... + \mathbf{A_n}\mathbf{x}(t-\tau_n)$$

Where $\mathbf{x}(t) \in \mathbb{R}^n$, $\mathbf{A_i} \in \mathbb{R}_{n,n}$ and $\tau_n > ... > \tau_1 > 0$.

Since the systems that appear in our project have a maximum number of three DDEs, we will only consider cases where the maximum number of different delays is three. This assumption will lead us to try to find a base of generalized eigenvectors such that the respective coefficient matrices diagonalise simultaneously and thus, reduce the system into decoupled scalar DDEs. Nonetheless, this base in general does not exist and as it will be proved later, that is the case in all the studied systems. Therefore, we will conclude the study of these systems with a numerical analysis.

Not being able to reduce the system into scalar DDEs does not imply that this system cannot be solved. There exist more advanced techniques to solve DDEs that may apply, unfortunately, they are not within the scope of this project.

With the motivation that under certain conditions most of the systems we will work with can be reduced into decoupled scalar DDEs, we will focus on this case to study the stability.

A **scalar delay differential equation with constant coefficients** can be expressed by:

$$\begin{aligned} \dot{x}(t) &= c_1 x(t) + c_2 x(t-\tau) \\ x(t) &= \psi(t) \quad \forall t < 0 \end{aligned}$$

Where $x(t) \in \mathbb{R}$, $c_1, c_2 \in \mathbb{R}$, $\tau > 0$ is the delay and $\psi \in \mathcal{C}(\mathbb{R}, \mathbb{R})$ is the function that provides the initial condition.

The are multiple ways to solve this equation, however not all of them are useful to study the stability.

With the motivation to understand better how delay differential equations function, we will briefly introduce the steps Method and the Method of Characteristics.

The steps Method

This iterative method is based on selecting an interval and transforming the DDE into an ODE using the history function for that interval. The resulting ODE is solved and the process is repeated on the next interval using the former solution as history function.

The intervals are usually segmented as $[t-\tau, t]$, so that the delayed term is every time known. More concisely, notice that in the interval $[-\tau, 0]$, the solution is given by $\psi(t)$. For the interval $[0, \tau]$, observe that the delayed term $x(t-\tau) = \psi(t-\tau)$ is also known, thus the equation becomes an ODE with initial condition $x(0) = \psi(0)$. This process can be repeated multiple times in order to calculate the solution within a time interval. Nevertheless, it is not possible to determine the stability with this method, thus we will not use this method.

Method of Characteristics

Assume the solution of the form $x(t) = ke^{mt}$, where k is a constant and $m \in \mathbb{C}$. Clearly the zero function is solution. Consider $k \neq 0$, the so-called **characteristic equation** immediately derives:

$$(m - c_1)e^{m\tau} = c_2$$

Observe that when $c_2 = 0$, which is the ODE case, the characteristic equation turns into $m = c_1$, which implies $x(t) = ke^{c_1 t}$. Certainly, this is the solution for the ODE $\dot{x}(t) = c_1 x(t)$.

If $c_1 \neq 0$ and $c_1 \neq 0$, we proceed with a change of variables $n := m - c_1$, which transforms the characteristic equation into:

$$ne^{n\tau} = c_2 e^{-\tau c_1} \Rightarrow n\tau e^{n\tau} = c_2 \tau e^{-\tau c_1}$$

We can use the Lambert Function [3], defined as the inverse of the complex function $f(z) = ze^z$, i.e. it satisfies $W(ze^z) = z$. Since f is not injective, the Lambert function is multivalued, except at 0. Then $n = \frac{W(c_2\tau e^{-\tau c_1})}{\tau}$. Observe that $W(c_2\tau e^{-\tau c_1})$ has an infinite number of complex roots. Moreover, if $c_2 < -\frac{1}{\tau e}$ it has no real roots, if $c_2 = -\frac{1}{\tau e}$ or $c_2 \geq 0$ there is one real root and lastly, if $-\frac{1}{\tau e} < c_2 < 0$, there are two real roots.

Lastly, if $c_1 = 0$ and $c_2 \neq 0$, which corresponds to the case of the purely delayed DDE, the characteristic equation implies:

$$m\tau e^{m\tau} = \tau c_2$$

In order to solve this equation, we can use the Lambert Function again and get $m = \frac{1}{\tau}W(c_2\tau)$, with an infinite number of complex solutions. We will not develop further this method since it will not be used for the stability study.

Stability of a scalar DDE

A first order scalar purely delayed Differential Equation has the following expression:

$$\dot{x}(t) = \lambda x(t - \tau)$$

For $x(t) \in \mathbb{R}$ and $\lambda \in \mathbb{R}$. The delay is represented by $\tau > 0$.

In order to study the stability of scalar purely delayed differential equations, we will follow the procedure in Chapter 2 of [1] and [2].

Remark 1.10. If $\lambda > 0$, the system is unstable independently of the delay value τ. The reason for this is that the ODE case with $\tau = 0$ would be already unstable. With respect to the ODE case, the delay introduces inestability. This means that if the ODE is already unstable, all the solutions to the DDE will be unstable. Moreover, if $\lambda = 0$, the solution is a constant. Thus, in order to find the stability boundary we will suppose $\lambda < 0$.

Begin by performing a convenient change of variables:

$$t' = \frac{t}{\tau} \Longrightarrow \frac{dx(t)}{dt} = \frac{dx(\tau t')}{dt'}\frac{1}{\tau}$$

After the change of variables, $\tau\lambda$ is the new control parameter.

$$\frac{dx(\tau t')}{dt'} = \tau\lambda x(\tau t' - \tau) \;\; \forall t' \geq 0 \Longrightarrow \frac{dx(t')}{dt'} = \tau\lambda x(t' - 1) \;\; \forall t' \geq 0$$

We can assume the solution can be written as a linear combination of exponential forms $x(t') = e^{mt'}x_0$, where $m \in \mathbb{C}$. By imposing the DDE at all times and for every initial condition, we get the characteristic equation:

$$(m - \tau\lambda e^{-m})e^{mt'}x_0 = 0 \quad \forall t' \geq 0, \forall x_0 \in \mathbb{R} \Longrightarrow m - \tau\lambda e^{-m} = 0$$

The characteristic equation admits several roots. To study the stability, we will separate the real part from the imaginary part of the equation. Thus, let $m = \alpha + i\beta$, $\alpha, \beta \in \mathbb{R}$. When $\alpha < 0$ and $\beta = 0$ the solution will be stable and non-oscillatory. When $\alpha < 0$ and $\beta \neq 0$, it will become oscillatory stable. Lastly, when $\alpha > 0$, the solution will be unstable.

Substituting into the characteristic equation and separating the resulting real and imaginary parts, we get two equations:

$$\alpha - \tau\lambda e^{-\alpha} cos(\beta) = 0$$

$$\beta + \tau\lambda e^{-\alpha} sin(\beta) = 0$$

As a consequence, α and β satisfy a parameter-free equation:

$$-\frac{\alpha}{\beta} = cot(\beta)$$

We can determine the value of α for which β becomes zero, which corresponds to the limit of oscillatory behaviour. Notice that by imposing $\beta = 0$ on the real part of the characteristic equation, we get $\alpha e^{\alpha} = \tau\lambda$, which can be solved using the Lambert W function, resulting in $\alpha = W(\lambda\tau)$. Nonetheless, in this case the limit of oscillatory behaviour can be computed directly from the parameter-free equation:

$$\lim_{\beta\to 0} \alpha = \lim_{\beta\to 0} -\beta cot(\beta) = \lim_{\beta\to 0} -\beta\frac{cos(\beta)}{sin(\beta)} = \lim_{\beta\to 0} \frac{-\beta}{\beta} = -1$$

This result implies that when $\alpha < -1$ solutions are stable non-oscillatory, while for $\alpha \in (-1, 0)$, they are oscillatory stable. Moreover, $\alpha = -1$ in the parameter-free equation implies $\beta = tan(\beta)$, which admits $\beta = 0$. This ensures the oscillatory transition occurs within the stable region.

We can define the **oscillatory limit** as the delay over which the solutions are oscillatory stable and underneath, non-oscillatory stable. We will denote it by $\tau_{oscil}(\lambda)$. By imposing $\alpha = -1$ and $\beta = 0$ on the real part of the characteristic equation, we get an explicit expression:

$$\tau\lambda = -\frac{1}{e} \Longrightarrow \tau_{oscil}(\lambda) := -\frac{1}{e\lambda}$$

The next step is to define the **stability limit**, defined as the delay over which the solutions are unstable and underneath, oscillatory stable. We will denote it by $\tau_{stabil}(\lambda)$. Imposing $\alpha = 0$ on the real part of the characteristic equation leads to:

$$0 = \tau\lambda cos(\beta) \implies \beta = (2k+1)\frac{\pi}{2} \quad \forall k \in \mathbb{Z}$$

Lastly, the imaginary part of the characteristic equation implies:

$$(2k+1)\frac{\pi}{2} = \tau\lambda(-1)^{k+1} \Rightarrow \tau = (-1)^{k+1}\frac{(2k+1)\pi}{2\lambda} = \left\{-\frac{\pi}{2\lambda}, +\frac{3\pi}{2\lambda}, ...\right\}$$

It is in our interest to study the behaviour of the system with small delays. Consequently, we will choose $k = 0, -1$, which corresponds to $\beta = \pm\frac{\pi}{2}$. Under these considerations, we get an expression for the stability limit:

$$\tau_{stabil}(\lambda) := -\frac{\pi}{2\lambda}$$

We will formalise this result with the following Proposition.

Proposition 1.11. *The oscillatory and stability limits of the delayed linear scalar DDE $\dot{x}(t) = \lambda x(t-\tau)$ with $\lambda < 0$ are defined as:*

$$\tau_{oscil}(\lambda) := -\frac{1}{e\lambda} \qquad \tau_{stabil}(\lambda) := -\frac{\pi}{2\lambda}$$

These definitions describe the boundaries of the stability or the oscillatory behaviour of the solution. More concisely:

If $\tau < -\frac{1}{e\lambda}$, solution is **non-oscillatory stable**.

If $-\frac{1}{e\lambda} < \tau < -\frac{\pi}{2\lambda}$, solution is **oscillatory stable**.

If $\tau > -\frac{\pi}{2\lambda}$, solution is **unstable**.

Remark 1.12. Observe that both limits are strictly positive due to $\lambda < 0$. As explained in Remark 1.10, in the case of $\lambda > 0$, the solutions are always unstable and thus, these limits are not defined.

We will generalise this Proposition to the case of a system of multiple decoupled linear scalar purely delayed differential equations system: $\dot{\mathbf{z}}(t) = \mathbf{D}\mathbf{z}(t-\tau)$, where $\mathbf{D}$ is a diagonal matrix. Notice that if $\mathbf{D}$ has at least one strictly positive diagonal entry, the system will be **unstable**, independently of τ. If all the entries are negative or zero, we can define the stability boundary through the generalized oscillatory and stability limits of the system.

Here we have defined the stability regions as intervals of τ. Let I_s be the stable non-oscillatory interval of the system, I_o the stable oscillatory and I_u the unstable, such that they form a partition of $\mathbb{R}_{>0}$. The stability region of the system corresponds to $I_s \cup I_o$, so that the unstable region is given by $I_u = \mathbb{R}_{>0} \backslash (I_s \cup I_o)$. Moreover, the oscillatory stable interval is given by $I_o = \mathbb{R}_{>0} \backslash (I_s \cup I_u)$.

On the one hand, the non-oscillatory stable region of the system I_s will be the intersection of the non-oscillatory stable regions of each DDE. On the other hand, the unstable region of the system will be the union of the unstable intervals of each DDE. This leads to the definition of the oscillatory stable region as the rest interval.

This reasoning translates into the following Proposition.

Proposition 1.13. *Let a system of n decoupled purely delayed DDEs $\dot{\mathbf{z}}(t) = \mathbf{D}\mathbf{z}(t-\tau)$, where $\mathbf{D}$ is a diagonal matrix with only negative or zero diagonal elements. The oscillatory and stability limits are defined as:*

$$\tau_{oscil} := \min_{\lambda_i < 0} \tau_{oscil}(\lambda_i) \qquad \tau_{stabil} := \min_{\lambda_i < 0} \tau_{stabil}(\lambda_i)$$

where λ_i, $i \in \{1, ..., n\}$ are the elements of the diagonal matrix $\mathbf{D}$. The stability of the system is determined by these limits and the delay value τ:

If $\tau < \tau_{oscil}$, the system is **non-oscillatory stable**.

If $\tau_{oscil} < \tau < \tau_{stabil}$, the system is **oscillatory stable**.

If $\tau > \tau_{stabil}$, the system is **unstable**.

Linearization a system of DDEs and non-delayed equations

We have defined the Elastic equilibrium from elastic Energy defined in equation (3). The final conclusion of sum of stress forces equals zero translates into a non-delayed equation, while the rest-length follows a delayed differential equation as stated in (2). This inspires the necessity to define linearisation of a system where purely delayed differential equations and non-delayed equations coexist.

Let $\mathbf{F}$ be a smooth function that describes a system of n variables and n equations. The variables, represented by $z_1, z_2, ..., z_n$, correspond to real functions dependent on time such that $z_i(t) \in \mathbb{R} \ \ \forall t \geq 0$. Assume that we know the initial state of the system is given by $\mathbf{z_0} \in \mathbb{R}^n$ and we wish to compute the linearisation of $\mathbf{F}$ at the initial conditions.

Moreover, consider an order of the indices of the system equations. We define $\Lambda \subseteq \{1, ..., n\}$ as the set of indices for the purely delayed differential equations. This definition implies that $\forall i \notin \Lambda$, the corresponding equation is non-delayed and non-differential.

Proposition 1.14. *The linearisation of* $\mathbf{F}$ *at* $\mathbf{z_0}$ *can be expressed as:*

$$\mathbf{F}(\mathbf{z}) \simeq \mathbf{F}(\mathbf{z_0}) + \sum_{1 \leq i,j \leq n} D\mathbf{F}(\mathbf{z_0})_{ij}(z_j(t - \delta_{i,\Lambda}\tau) - z_j(0))$$

Where Λ *is the set of indices for the delayed equations in the system and:*

$$\delta_{i,\Lambda} := \begin{cases} 1 \text{ if } i \in \Lambda, \text{ i.e. the i-th equation is a purely delayed differential equation} \\ 0 \text{ if } i \notin \Lambda, \text{ i.e. the i-th equation is non-delayed} \end{cases}$$

Proof. Consider the equations indexed by $i \in \Lambda$ and $j \notin \Lambda$. Let g_i and g_j be the functions such that the equation i can be expressed by $g_i(t - \tau) = 0$ and the equation j, by $g_j(t) = 0$. The linearisation of each equation at the initial condition is:

$$g_i(t - \tau) \simeq g_i(0) + \nabla g_i\Big|_{t=0} \cdot (\mathbf{z}(t - \tau) - \mathbf{z}_0)$$
$$g_j(t) \simeq g_j(0) + \nabla g_j\Big|_{t=0} \cdot (\mathbf{z}(t) - \mathbf{z}_0)$$

Where $\nabla = (\partial_{z_1}, ..., \partial_{z_n})$ is the gradient. Linearising every equation leads to:

$$\begin{bmatrix} g_1(t - \delta_{1,\Lambda}\tau) \\ \vdots \\ g_n(t - \delta_{1,\Lambda}\tau) \end{bmatrix} = \begin{bmatrix} g_1(0) \\ \vdots \\ g_n(0) \end{bmatrix} + \begin{bmatrix} \partial_{z_1} g_1(0) & ... & \partial_{z_n} g_1(0) \\ \vdots & & \vdots \\ \partial_{z_1} g_n(0) & ... & \partial_{z_n} g_n(0) \end{bmatrix} \begin{bmatrix} z_1(t - \delta_{1,\Lambda}\tau) - z_1(0) \\ \vdots \\ z_n(t - \delta_{1,\Lambda}\tau) - z_n(0) \end{bmatrix}$$

Which corresponds to the expression given in the statement of the Proposition.

Observe that this is only possible if the initial condition of the DDE is constant, since $\mathbf{z}(t) = \mathbf{z_0} \ \forall t \leq 0$. This is the case of the rest-length evolution equation in (2) and thus, it will be the case of all the DDEs in our project.

Remark 1.15. In the case of multiple delays, it is also possible to linearise the system following Proposition 1.14:

$$\mathbf{F}(\mathbf{z}) \simeq \mathbf{F}(\mathbf{z_0}) + \sum_{1 \leq i,j \leq n} D\mathbf{F}(\mathbf{z_0})_{ij}(z_j(t - \delta_{i,\Lambda}\tau_i) - z_j(0))$$

2. Methodology

In this section, we will study two models for oscillations in biological tissues under the assumptions and the laws explained in the Introduction.

2.1 First Model

Consider a strip of tissue where cells are adjacent to each other. Assume a horizontal displacement $\mathbf{u}(t)$ acting on the superior and inferior nodes of each cell in a anti-phase fashion, like in the following diagram:

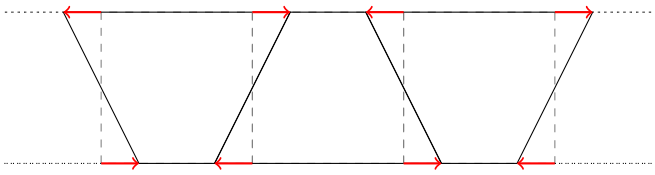

Figure 1: A section of tissue under the displacement $\mathbf{u}(t)$ -in red-. The dashed-line refers to the initial rest state.

Remark 2.1. Due to displacement only being horizontal and the assumption of constant height, the walls can only stretch or shrink without vertical movement.

As it was mentioned in the Introduction, the displacement induces stress forces $\sigma(t)$ on each edge. Thus, to understand the deformation at each instant t, we can focus on how the stress forces act on each node, i.e. the intersection of edges. For this purpose, we will impose mechanical equilibrium at each node. The reasons behind this are the symmetry of the displacement and Remark 2.1.

For instance, take the central cell superior left vertex of Fig. 1. Then, we have the following force diagram:

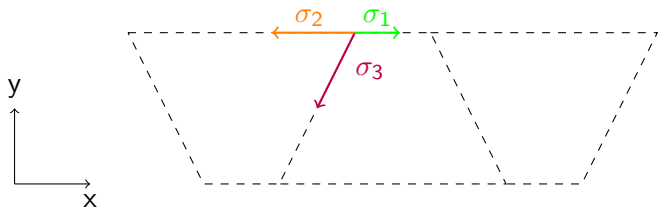

Figure 2: Force diagram at the superior left node, intersection of edges 1,2 and 3. The stress force induced by displacement on edge i is represented by $\sigma_i(t)$, following the definition in (1).

It is sufficient to impose horizontal equilibrium, given that there is no vertical deformation. This does not imply that the vertical component of $\sigma_3(t)$ is zero. It is actually compensated by the stress force on the inferior node.

The mechanical equilibrium condition is:

$$\sigma_1(t) - \sigma_2(t) - \sigma_3(t)sin(\alpha(t)) = 0 \tag{4}$$

Where $\alpha(t)$ is the angle between the vertical axis and $\sigma_3(t)$, which can be determined as the following diagram illustrates:

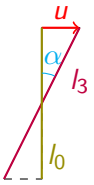

Figure 3: Geometrical condition which allows the definition of $\alpha(t)$. l_0 is the constant height and $l_3(t)$ is the deformed length of edge 3.

From Fig. 3, we find an expression for the angle.

$$u(t) = \frac{1}{2}l_3(t)sin(\alpha(t)) \Rightarrow \alpha(t) := arcsin\left(\frac{2u(t)}{l_3(t)}\right) \tag{5}$$

Together with the definition of stress force given in the Introduction, the equilibrium condition writes:

$$0 = l_1(t) - L_1(t) - l_2(t) + L_2(t) - 2u(t) + \frac{2u(t)L_3(t)}{l_3(t)} \tag{6}$$

Remark 2.2. Notice how this condition does not depend on the stiffness k. This is due to k being a strictly positive constant and the hypothesis of all the cell walls having the same stiffness. Also observe that it coincides with the expression for equilibrium given in the Introduction.

Also from Fig. 3, we find an expression for $l_3(t)$:

$$l_3(t) = \sqrt{l_0^2 + 4u^2(t)} \quad \forall t \in \mathbb{R} \tag{7}$$

Lastly, from the symmetry in Fig. 1, we can also find explicit expressions for $l_1(t)$ and $l_2(t)$.

$$l_1(t) = l_0 - 2u(t), \quad l_2(t) = l_0 + 2u(t) \quad \Longrightarrow \quad l_1(t) + l_2(t) = 2l_0 \quad \forall t \tag{8}$$

Remark 2.3. These geometrical conditions also delimit the range of definition of the displacement. Effectively, since $l_i(t)$ must be positive, it is necessary that $\|u(t)\| < \frac{l_0}{2}\ \forall t$.

All the deformed lengths depend on $u(t)$, which is dependant on the rest-lengths through the equilibrium condition. Besides, each of the rest-lengths of the three edges satisfy the delay differential equation in (2):

$$\begin{cases} \dot{L_1}(t) = \gamma(l_1(t-\tau) - L_1(t-\tau)) \\ \dot{L_2}(t) = \gamma(l_2(t-\tau) - L_2(t-\tau)) \\ \dot{L_3}(t) = \gamma(l_3(t-\tau) - L_3(t-\tau)) \end{cases} \tag{9}$$

We can add the equilibrium equation and the geometrical conditions to get a 4-dimensional non-linear determined system:

$$\begin{cases} \dot{L_1}(t) = \gamma(l_0 - 2u(t-\tau) - L_1(t-\tau)) \\ \dot{L_2}(t) = \gamma(l_0 + 2u(t-\tau) - L_2(t-\tau)) \\ \dot{L_3}(t) = \gamma\left(\sqrt{l_0^2 + 4u^2(t-\tau)} - L_3(t-\tau)\right) \\ 0 = L_2(t) - L_1(t) - 6u(t) + \dfrac{2u(t)L_3(t)}{\sqrt{l_0^2 + 4u^2(t)}} \end{cases} \tag{10}$$

This system can be further reduced by introducing a new variable $\psi(t) := L_1(t) - L_2(t)$. For this development, we will use the notation $z = z(t)$ and $z_\tau := z(t-\tau)\ \forall z \in \mathcal{C}(\mathbb{R})$. We can define a new system in terms of ψ, u and L_3:

$$\begin{cases} \dot{L_3} = \gamma\left(\sqrt{l_0^2 + 4u_\tau^2} - L_{3\tau}\right) \\ \dot{\psi} = -\gamma(4u_\tau + \psi_\tau) \\ \psi = -6u + \dfrac{2uL_3}{\sqrt{l_0^2 + 4u^2}} \end{cases} \tag{11}$$

Last equation implies:

$$\dot{\psi} = -6\dot{u} + 2\frac{\dot{u}L_3 + u\dot{L_3}}{\sqrt{l_0^2 + 4u^2}} - 8\frac{\dot{u}L_3u^2}{\left(l_0^2 + 4u^2\right)^{3/2}}$$

This equation must be equal to the second one in the system (11), leading to:

$$-3\dot{u} + \frac{\dot{u}L_3}{\sqrt{l_0^2 + 4u^2}} - 4\frac{\dot{u}L_3u^2}{\left(l_0^2 + 4u^2\right)^{3/2}} + \frac{u\dot{L_3}}{\sqrt{l_0^2 + 4u^2}} = \gamma u_\tau - \gamma\frac{u_\tau L_{3\tau}}{\sqrt{l_0^2 + 4u_\tau^2}}$$

Using the expression for $\dot{L_3}$, we get:

$$-3\dot{u} + \frac{\dot{u}L_3}{\sqrt{l_0^2 + 4u^2}} - 4\frac{\dot{u}L_3u^2}{\left(l_0^2 + 4u^2\right)^{3/2}} + \gamma\frac{u\sqrt{l_0^2 + 4u_\tau^2}}{\sqrt{l_0^2 + 4u^2}} - \gamma\frac{uL_{3\tau}}{\sqrt{l_0^2 + 4u^2}} = \gamma u_\tau - \gamma\frac{u_\tau L_{3\tau}}{\sqrt{l_0^2 + 4u_\tau^2}}$$

Which eventually turns into the DDE:

$$\dot{u} = \gamma\frac{u_\tau\left(1 - \dfrac{L_{3\tau}}{\sqrt{l_0^2 + 4u_\tau^2}}\right) - u\left(\dfrac{\sqrt{l_0^2 + 4u_\tau^2} - L_{3\tau}}{\sqrt{l_0 + 4u^2}}\right)}{\left(\dfrac{L_3l_0^2}{\left(l_0^2 + 4u^2\right)^{3/2}} - 3\right)}$$

Conclusively, the system in (10) is equivalent to the following 3-dimensional non-linear system:

$$\begin{cases} \dot{L_1} = \gamma(l_0 - 2u_\tau - L_{1\tau}) \\ \dot{L_3} = \gamma\left(\sqrt{l_0^2 + 4u_\tau^2} - L_{3\tau}\right) \\ \dot{u} = \gamma \dfrac{u_\tau\left(1 - \dfrac{L_{3\tau}}{\sqrt{l_0^2 + 4u_\tau^2}}\right) - u\left(\dfrac{\sqrt{l_0^2 + 4u_\tau^2} - L_{3\tau}}{\sqrt{l_0 + 4u^2}}\right)}{\left(\dfrac{L_3 l_0^2}{\left(l_0^2 + 4u^2\right)^{3/2}} - 3\right)} \end{cases} \tag{12}$$

Remark 2.4. Notice that from system (11), we have an expression for $L_2 = L_1 + 6u - \frac{2uL_3}{\sqrt{l_0^2+4u^2}}$.

Remark 2.5. From a numerical point of view, the first equation of system (12) is a post-process of the other two. This means that it is possible to firstly solve the two-dimensional system and use the solution to solve the first equation.

For simplicity purposes in the analytic study we will proceed with system in (10).

Initial conditions

Before moving on to the analysis, we must set the initial data for our variables. We introduce two dimensionless parameters m_u and m_L, ratios of the height l_0, such that:

$$L_0 := L_3(0) = m_L l_0, \qquad u(0) = m_u l_0$$

Initially, the deformed lengths must satisfy the geometrical conditions, thus:

$$l_1(0) = l_0(1 - 2m_u), \qquad l_2(0) = l_0(1 + 2m_u), \qquad l_3(0) = l_0(\sqrt{1 + 4m_u^2}) \tag{13}$$

Besides, in order to guarantee the equilibrium initially we introduce a small perturbation ϵ such that:

$$L_1(0) = m_L l_0, \qquad L_2(0) = m_L l_0 + \epsilon, \qquad L_3(0) = m_L l_0 \tag{14}$$

By imposing the equilibrium equation, we obtain an expression for ϵ:

$$\epsilon = \epsilon(l_0, m_L, m_u) := 2m_u l_0\left(3 - \frac{m_L}{\sqrt{1 + 4m_u^2}}\right) \tag{15}$$

Remark 2.6. We can define the range of definition of these parameters. By (13), since the deformed length is always positive, $m_u \in [-\frac{1}{2}, \frac{1}{2}]$. By (14), $m_L \geq 0$. If $m_L > 1$, the rest length of each edge is greater than the respective deformed length, $L_i(0) > l_i(0)$. This corresponds to the case where cells are initially dilated. On the contrary, $m_L < 1$ refers to the cells being initially contracted. It has been empirically observed that cells are initially contracted. For example, in wound healing the cell pressure is fundamental for the control of the process [7]. Therefore, we will set $m_L \in [0, 1]$.

Lastly, we must make sure that ϵ is well-defined in the domain given by the definition intervals of the parameters and that its value does not conflict with the definition of L_2, which should always be positive. The following plot shows the area where $\epsilon < 0$. Its value will not lead to conflicts since this area does not intersect with the domain of the parameters.

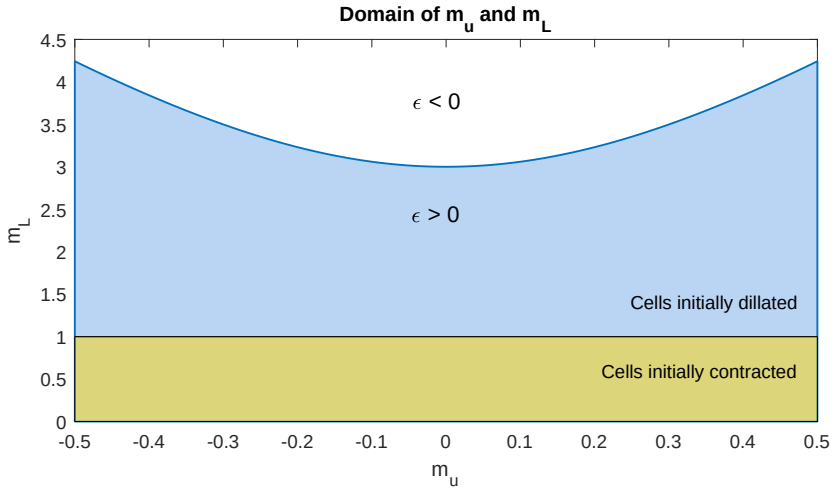

Figure 4: Curve -in blue- such that $\epsilon = 0$, i.e. $m_L = \sqrt{1+4m_u^2}$. Underneath, $\epsilon > 0$. In yellow, the domain for which cells are initially contracted. The area in blue and white corresponds to initially enlarged cells. Observe that for initially contracted cells, ϵ is always positive.

2.1.1 Linear Analysis

This analysis focuses on the non-linear system in (10), given the initial conditions in (14) and $u(0) = m_u l_0$. In a non-linear ODE system, the general procedure to determine the stability is to linearise the system and diagonalise the resulting system matrix. The eigenvalues determine the stability of the system as stated in Proposition 1.9. Nonetheless, in the case of Delay Differential Equations, the study of stability becomes much more complicated. For instance, the case of the first-order linear scalar pure DDE, as stated in Proposition 1.11, requires both the leading coefficient and the delay in order to determine the stability.

With the purpose of studying the stability of the system in (10), we will proceed to linearise it at the initial conditions. Our final intention is to reduce the system into scalar decoupled DDEs, the stability of which has already been studied in the Introduction.

By Proposition 1.14, the linearised system at the initial condition is:

$$\begin{cases} \dot{L_1}(t) = \gamma(l_0 - 2u(t-\tau) - L_1(t-\tau)) \\ \dot{L_2}(t) = \gamma(l_0 + 2u(t-\tau) - L_2(t-\tau)) \\ \dot{L_3}(t) = \gamma\left(\dfrac{l_0}{\sqrt{1+4m_u^2}} + \dfrac{4m_u}{\sqrt{1+4m_u^2}}u(t-\tau) - L_3(t-\tau)\right) \\ 0 = -\dfrac{2m_L m_u l_0}{(1+4m_u^2)^{\frac{3}{2}}} - L_1(t) + L_2(t) + \dfrac{2m_u}{\sqrt{1+4m_u^2}}L_3(t) + \left(-6 + \dfrac{2m_L}{(1+4m_u^2)^{\frac{3}{2}}}\right)u(t) \end{cases} \tag{16}$$

The development and computations can be found in Appendix A.1.

Remark 2.7. Notice that l_0 only appears in the constant coefficients. This means that the stability of the system does not depend on l_0. Since the coefficients of the variables depend on m_u, m_L and γ, these three

parameters will determine the stability of the system with $\tau = 0$ (ODE).

Remark 2.8. Observe that $\epsilon > 0$ implies $3 > \frac{m_L}{\sqrt{1+4m_u^2}}$. Then, $3(1+4m_u^2)^{\frac{3}{2}} > m_L(1+4m_u^2) \geq m_L$, which proves that the coefficient of $u(t)$ in the equilibrium equation is non-zero, i.e. the equilibrium always depends on the displacement.

From the last equation, an explicit expression for $u(t)$ $\forall t$ can be derived. This is possible thanks to Remark 2.8.

$$u(t) = \frac{m_L m_u l_0}{m_L - 3(1+4m_u^2)^{\frac{3}{2}}} + \frac{(1+4m_u^2)^{\frac{3}{2}}}{6(1+4m_u^2)^{\frac{3}{2}} - 2m_L}(L_2(t) - L_1(t)) + \frac{m_u + 4m_u^3}{3(1+4m_u^2)^{\frac{3}{2}} - m_L}L_3(t) \tag{17}$$

This is a non-delayed equation which is valid $\forall t \in \mathbb{R}$. Therefore, the expression for $u(t-\tau)$ can be used to reduce the former system into a 3-dimensional purely delayed system.

$$\begin{bmatrix} \dot{L}_1(t) \\ \dot{L}_2(t) \\ \dot{L}_3(t) \end{bmatrix} = \begin{bmatrix} A & B & C \\ B & A & -C \\ C & -C & D \end{bmatrix} \begin{bmatrix} L_1(t-\tau) \\ L_2(t-\tau) \\ L_3(t-\tau) \end{bmatrix} + \gamma l_0 \begin{bmatrix} 1 + \dfrac{2m_L m_u}{3(1+4m_u^2)^{\frac{3}{2}} - m_L} \\ 1 - \dfrac{2m_L m_u}{3(1+4m_u^2)^{\frac{3}{2}} - m_L} \\ \dfrac{1}{\sqrt{1+4m_u^2}}\left(1 - \dfrac{4m_u^2 m_L}{3(1+4m_u^2)^{\frac{3}{2}} - m_L}\right) \end{bmatrix} \tag{18}$$

Where:

$$A := \gamma \frac{m_L - 2\left(1+4m_u^2\right)^{\frac{3}{2}}}{3(1+4m_u^2)^{\frac{3}{2}} - m_L} \qquad B := -\gamma \frac{\left(1+4m_u^2\right)^{\frac{3}{2}}}{3(1+4m_u^2)^{\frac{3}{2}} - m_L}$$

$$C := -\gamma \frac{2m_u(1+4m_u^2)}{3(1+4m_u^2)^{\frac{3}{2}} - m_L} \qquad D := \gamma \frac{m_L - \sqrt{1+4m_u^2}(3+8m_u^2)}{3(1+4m_u^2)^{\frac{3}{2}} - m_L}$$

Besides, these matrix entries satisfy the following relations:

$$A + B = -\gamma, \qquad C = \frac{2m_u B}{\sqrt{1+4m_u^2}}, \qquad D = -\gamma - \frac{C^2}{B}$$

Remark 2.9. In case of different delays, let τ_1, τ_2, τ_3 be the delays of first, second and third equation of (16), respectively. The deduction of the 3-dimensional system is also valid in this case. The linearisation with multiple delay is specified in Remark 1.15. Then, by substituting the expression for $u(t-\tau_i)$ at the i-th equation, the same reduced system is deduced.

Uniform delay

Suppose the delay is the same for all the equations. Since the system is linear, we proceed to diagonalise the system matrix. Firstly, we calculate the characteristic polynomial, the roots of which correspond to the eigenvalues of the matrix:

$$0 = \begin{vmatrix} -\gamma - B - \lambda & B & C \\ B & -\gamma - B - \lambda & -C \\ C & -C & -\gamma - \frac{C^2}{B} - \lambda \end{vmatrix} = (\gamma + \lambda)^2 \left(-2B - \frac{C^2}{B} - \gamma - \lambda\right)$$

The eigenvalues of the system matrix are:

$$\lambda_{1,3} = -\gamma, \qquad \lambda_2 = \gamma \frac{m_L - \sqrt{1+4m_u^2}(3+8m_u^2) + 2(1+4m_u^2)^{\frac{3}{2}}}{3(1+4m_u^2)^{\frac{3}{2}} - m_L}$$

Remark 2.10. The first double eigenvalue is real and negative since $\gamma \in \mathbb{R}_{>0}$. The second eigenvalue is also real but its sign depends on the initial conditions. Nevertheless, as it can be observed in Figure 5, λ_2 is always negative within the domain of definition for m_u and m_L. From this observation we conclude that the linearised system in (18) with $\tau = 0$ is stable non-oscillatory.

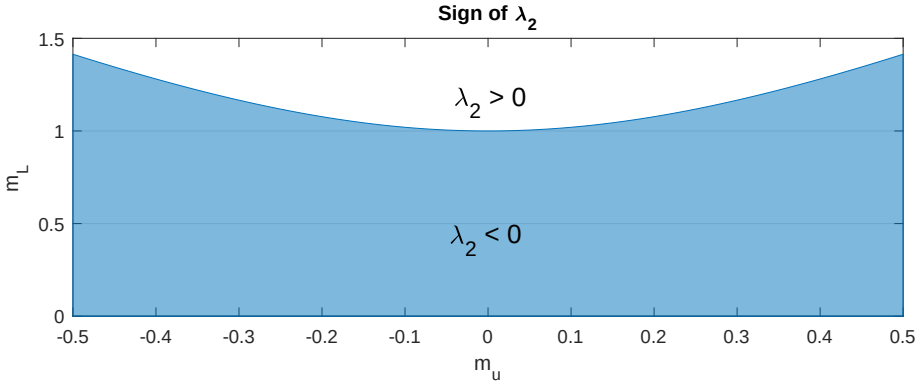

Figure 5: Curve such that $\lambda_2 = 0$. The area underneath represents the region where $\lambda_2 < 0$ and the ODE system is stable. Observe that within our domain of definition for m_u and m_L, λ_2 is always negative.

The eigenvectors of the system matrix correspond to the generators of the subspaces $\ker(M - \lambda Id)$, where M is the system matrix and λ is an eigenvalue. More concisely, the three eigenvectors $\mathbf{v_1}, \mathbf{v_2}, \mathbf{v_3}$ are such that:

$$\ker(M + \gamma Id) =< \mathbf{v_1}, \mathbf{v_3} > \quad \text{and} \quad \ker(M - \lambda_2 Id) =< \mathbf{v_2} >$$

The result is the following:

$$\mathbf{v_1} = \begin{pmatrix} 1 \\ 1 \\ 0 \end{pmatrix}, \quad \mathbf{v_2} = \begin{pmatrix} -\frac{B}{C} \\ \frac{B}{C} \\ 1 \end{pmatrix} = \begin{pmatrix} -\frac{\sqrt{1+4m_u^2}}{2m_u} \\ \frac{\sqrt{1+4m_u^2}}{2m_u} \\ 1 \end{pmatrix}, \quad \mathbf{v_3} = \begin{pmatrix} \frac{C}{B} \\ 0 \\ 1 \end{pmatrix} = \begin{pmatrix} \frac{2m_u}{\sqrt{1+4m_u^2}} \\ 0 \\ 1 \end{pmatrix} \tag{19}$$

Remark 2.11. Notice how m_L does not affect the eigenvectors but the eigenvalues. This means that the initial level of contraction will affect the intensity with which the deformation will take place but not the direction. In contrast, m_u -the initial displacement- affects both.

We can interpret the eigenvectors using Fig. 6. The signs in each eigenvector are arbitrarily chosen, consequently the aim of this interpretation is to determine which simultaneous deformation modes -also known as eigenmodes- take place. Observe that the factor $\sqrt{1+4m_u^2} \geq 1$. The possible deformation modes are:

(i) The first eigenmode, related to $\mathbf{v_1}$ and with associated eigenvalue $-\gamma$, corresponds to the case when L_1 and L_2 increase or decrease at the same pace, while L_3 stays constant.

(ii) The second eigenmode, related to $\mathbf{v_2}$ and with associated eigenvalue λ_2, corresponds to the case when L_2 increases at the same pace as L_1 decreases, while L_3 also increases at lower pace. The same reasoning is possible with decreasing instead of increasing.

(iii) The third eigenmode, related to $\mathbf{v_3}$ and with associated eigenvalue $-\gamma$, corresponds to the case when L_1 and L_3 increase or decrease, with L_3 at faster pace than L_1, while L_2 stays constant.

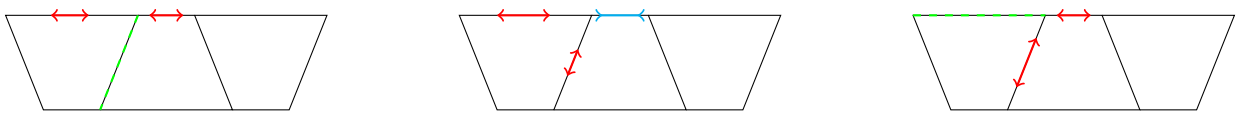

$\mathbf{v_1}, \quad -\gamma$ $\qquad$ $\mathbf{v_2}, \quad -\lambda_2$ $\qquad$ $\mathbf{v_3}, \quad -\gamma$

Figure 6: Interpretation of the eigenvectors. Below each figure, the related eigenvector and the associated eigenvalue. The red and blue arrows refer to the increase and decrease of the rest-length, respectively. The green dashed line refers to the steady rest-length.

In Remark 2.10, we have concluded that the system in (18) when $\tau = 0$ is stable non-oscillatory. However, this does not necessarily imply the stability of the system with delay. We will study this stability in the next paragraphs.

Firstly, let $\mathbf{M}$ be the system matrix and consider the matrix of eigenvectors $\mathbf{V}$ and the diagonal matrix of eigenvalues $\mathbf{D}$ defined as:

$$V := \begin{bmatrix} 1 & -\frac{\sqrt{1+4m_u^2}}{2m_u} & \frac{2m_u}{\sqrt{1+4m_u^2}} \\ 1 & \frac{\sqrt{1+4m_u^2}}{2m_u} & 0 \\ 0 & 1 & 1 \end{bmatrix} \qquad D := \begin{bmatrix} -\gamma & 0 & 0 \\ 0 & \gamma\frac{m_L-\sqrt{1+4m_u^2}(3+8m_u^2)+2(1+4m_u^2)^{\frac{3}{2}}}{3(1+4m_u^2)^{\frac{3}{2}}-m_L} & 0 \\ 0 & 0 & -\gamma \end{bmatrix}$$

Since $\mathbf{M}$ is symmetric, $\mathbf{V}$ is orthogonal and we have the decomposition $\mathbf{M} = \mathbf{V}\mathbf{D}\mathbf{V}^T$. For the stability analysis we will ignore the constant term of (18). Then, the homogeneous system can be expressed as:

$$\mathbf{V}^T \begin{bmatrix} \dot{L_1}(t) \\ \dot{L_2}(t) \\ \dot{L_3}(t) \end{bmatrix} = \mathbf{D}\mathbf{V}^T \begin{bmatrix} L_1(t-\tau_1) \\ L_2(t-\tau_2) \\ L_3(t-\tau_3) \end{bmatrix} \tag{20}$$

By defining a change of variables $\mathbf{z}(t) := \mathbf{V}^T\mathbf{L}(t) \in \mathbb{R}^3$, the former system becomes three decoupled linear scalar delay differential equations:

$$\begin{bmatrix} \dot{z_1}(t) \\ \dot{z_2}(t) \\ \dot{z_3}(t) \end{bmatrix} = \begin{bmatrix} \lambda_1 & 0 & 0 \\ 0 & \lambda_2 & 0 \\ 0 & 0 & \lambda_3 \end{bmatrix} \begin{bmatrix} z_1(t-\tau_1) \\ z_2(t-\tau_2) \\ z_3(t-\tau_3) \end{bmatrix} \tag{21}$$

In Proposition 1.11 the stability of this type of DDE has been studied. Following the nomenclature

used in the Proposition, we define the oscillatory and stability limits for each equation:

$$\tau_{oscil}(\lambda_{1,3}) := \frac{1}{e\gamma} \qquad \tau_{oscil}(\lambda_2) := \frac{m_L - 3(1+4m_u^2)^{\frac{3}{2}}}{e\gamma\left(m_L - \sqrt{1+4m_u^2}(3+8m_u^2) + 2(1+4m_u^2)^{\frac{3}{2}}\right)}$$

$$\tau_{stabil}(\lambda_{1,3}) := \frac{\pi}{2\gamma} \qquad \tau_{stabil}(\lambda_2) := \frac{\pi\left(m_L - 3(1+4m_u^2)^{\frac{3}{2}}\right)}{2\gamma\left(m_L - \sqrt{1+4m_u^2}(3+8m_u^2) + 2(1+4m_u^2)^{\frac{3}{2}}\right)}$$

Besides, by Proposition 1.13, the oscillatory and stability limits of the system (21) are defined as the minimum of the oscillatory and stability limits of each DDE, respectively. Consequently, the following lemma defines the stability boundaries.

Lemma 2.12. *The oscillatory behaviour and the stability of the system in (21) are exclusively determined by τ and γ by the following expressions:*

$$\tau_{oscil} = \frac{1}{e\gamma} \qquad \tau_{stabil} = \frac{\pi}{2\gamma}$$

Therefore, the initial conditions m_u, m_L within the definition domain do not affect the stability of the system.

Proof. We want to prove that, within the initial conditions domain, the minimum of the oscillatory and stability limits are $\tau_{oscil}(\lambda_{1,3})$ and $\tau_{stabil}(\lambda_{1,3})$, respectively. Then, it is sufficient to prove:

$$\frac{m_L - 3(1+4m_u^2)^{\frac{3}{2}}}{m_L - \sqrt{1+4m_u^2}(3+8m_u^2) + 2(1+4m_u^2)^{\frac{3}{2}}} \geq 1, \qquad \forall m_u \in \left(-\frac{1}{2}, \frac{1}{2}\right),\ \forall m_L \in (0,1)$$

Observe that the numerator is clearly negative and the quocient is positive due to $\lambda_2 < 0$. Thus, the denominator is also negative. The former inequality becomes:

$$m_L - 3(1+4m_u^2)^{\frac{3}{2}} \leq m_L - \sqrt{1+4m_u^2}(3+8m_u^2) + 2(1+4m_u^2)^{\frac{3}{2}} \Leftrightarrow 3 \geq \frac{3+8m_u^2}{1+4m_u^2} - 2 \Leftrightarrow 3 \geq \frac{1}{1+4m_u^2}$$

Lastly, this last inequality is satisfied due to $1 + 4m_u^2 \geq 1$. □

Conclusively, the stability boundaries of system (21) are defined with respect to τ and γ through the following expressions, which are graphically represented in Fig. 7.

(i) The system is **non-oscillatory stable** if $\tau < \dfrac{1}{e\gamma}$

(ii) The system is **oscillatory stable** if $\dfrac{1}{e\gamma} < \tau < \frac{\pi}{2\gamma}$

(iii) The system is **unstable** if $\tau > \dfrac{\pi}{2\gamma}$

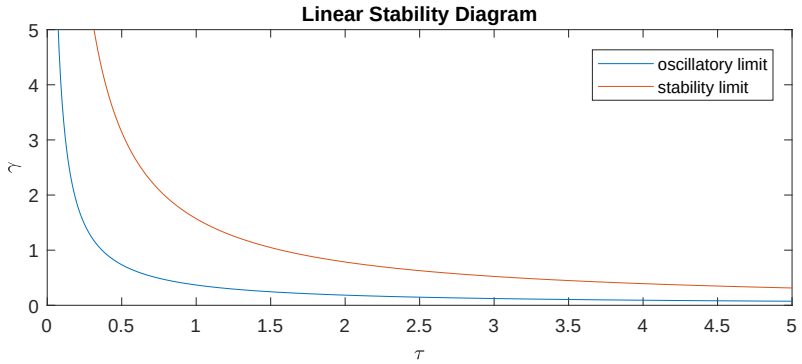

Figure 7: Oscillatory -orange- and Stability -blue- Limits, in blue and orange respectively. The system is stable non-oscillatory for all pairs of values under the blue curve, oscillatory stable in-between the curves and unstable over the orange curve.

Multiple delays

The deduction of system (18) is also valid considering different delays, as explained in Remark 2.9. Consider the following homogeneous purely delayed differential equations system:

$$\begin{bmatrix} \dot{L}_1(t) \\ \dot{L}_2(t) \\ \dot{L}_3(t) \end{bmatrix} = \begin{bmatrix} A & B & C \\ B & A & -C \\ C & -C & D \end{bmatrix} \begin{bmatrix} L_1(t-\tau_1) \\ L_2(t-\tau_2) \\ L_3(t-\tau_3) \end{bmatrix}$$

The purpose of this section is to diagonalise this system such that it becomes a system of three decoupled scalar DDE's. Since the delays are different, the diagonalisation is not direct and we must solve a problem of simultaneous diagonalisation.

For this development, we will simplify the notation by $\mathbf{z}(t) := \begin{bmatrix} L_1(t) \\ L_2(t) \\ L_3(t) \end{bmatrix}$.

Firstly, we split the system matrix into three new sparse matrices:

$$A_1 = \begin{bmatrix} A & 0 & 0 \\ B & 0 & 0 \\ C & 0 & 0 \end{bmatrix} \quad A_2 = \begin{bmatrix} 0 & B & 0 \\ 0 & A & 0 \\ 0 & -C & 0 \end{bmatrix} \quad A_3 = \begin{bmatrix} 0 & 0 & C \\ 0 & 0 & -C \\ 0 & 0 & D \end{bmatrix}$$

Such that

$$\begin{bmatrix} \dot{L}_1(t) \\ \dot{L}_2(t) \\ \dot{L}_3(t) \end{bmatrix} = \begin{bmatrix} A & B & C \\ B & A & -C \\ C & -C & D \end{bmatrix} \begin{bmatrix} L_1(t-\tau_1) \\ L_2(t-\tau_2) \\ L_3(t-\tau_3) \end{bmatrix} =$$

$$= \begin{bmatrix} A & 0 & 0 \\ B & 0 & 0 \\ C & 0 & 0 \end{bmatrix} \begin{bmatrix} L_1(t-\tau_1) \\ L_2(t-\tau_1) \\ L_3(t-\tau_1) \end{bmatrix} + \begin{bmatrix} 0 & B & 0 \\ 0 & A & 0 \\ 0 & -C & 0 \end{bmatrix} \begin{bmatrix} L_1(t-\tau_2) \\ L_2(t-\tau_2) \\ L_3(t-\tau_2) \end{bmatrix} + \begin{bmatrix} 0 & 0 & C \\ 0 & 0 & -C \\ 0 & 0 & D \end{bmatrix} \begin{bmatrix} L_1(t-\tau_3) \\ L_2(t-\tau_3) \\ L_3(t-\tau_3) \end{bmatrix}$$

In compact form, the equation can be expressed:

$$\dot{\mathbf{z}}(t) = A_1\mathbf{z}(t-\tau_1) + A_2\mathbf{z}(t-\tau_2) + A_3\mathbf{z}(t-\tau_3) \tag{22}$$

We will prove that there does not exist any base of generalised eigenvectors of A_1, A_2, A_3 such that it diagonalises each of the three matrices simultaneously. Equivalently, there does not exist three linearly independent generalised eigenvectors.

The eigenvalues of the respective matrices are the following:

A_1	A_2	A_3
$\lambda_1 = A$	$\gamma_1 = A$	$\rho_1 = D$
$\lambda_2 = 0$	$\gamma_2 = 0$	$\rho_2 = 0$
$\lambda_3 = 0$	$\gamma_3 = 0$	$\rho_3 = 0$

Table 1: Eigenvalues of the matrices

Suppose that the base of generalized eigenvectors exists. Let S be the matrix of eigenvectors. Then, equation (22) satisfies:

$$\dot{\mathbf{z}}(t) = S \begin{bmatrix} A & 0 & 0 \\ 0 & 0 & 0 \\ 0 & 0 & 0 \end{bmatrix} S^{-1}\mathbf{z}(t-\tau_1) + S \begin{bmatrix} 0 & 0 & 0 \\ 0 & A & 0 \\ 0 & 0 & 0 \end{bmatrix} S^{-1}\mathbf{z}(t-\tau_2) + S \begin{bmatrix} 0 & 0 & 0 \\ 0 & 0 & 0 \\ 0 & 0 & D \end{bmatrix} S^{-1}\mathbf{z}(t-\tau_3)$$

Then, by defining a change of variables $\boldsymbol{\xi}(t) := S^{-1}\mathbf{z}(t)$:

$$\dot{\boldsymbol{\xi}}(t) = \begin{bmatrix} A & 0 & 0 \\ 0 & 0 & 0 \\ 0 & 0 & 0 \end{bmatrix} \boldsymbol{\xi}(t-\tau_1) + \begin{bmatrix} 0 & 0 & 0 \\ 0 & A & 0 \\ 0 & 0 & 0 \end{bmatrix} \boldsymbol{\xi}(t-\tau_2) + \begin{bmatrix} 0 & 0 & 0 \\ 0 & 0 & 0 \\ 0 & 0 & D \end{bmatrix} \boldsymbol{\xi}(t-\tau_3)$$

Then, each component independently satisfies a scalar delay differential equation:

$$\implies \begin{cases} \dot{\xi}_1(t) = A\xi_1(t-\tau_1) \\ \dot{\xi}_2(t) = A\xi_2(t-\tau_2) \\ \dot{\xi}_3(t) = D\xi_3(t-\tau_3) \end{cases}$$

The stability and oscillatory behaviour of this type of DDE is studied and determined in Proposition 1.11.

Let $\mathbf{v} \in \mathbb{R}^3$ be a generalized eigenvector. Equivalently, $\mathbf{v}$ is an eigenvector of each matrix and thus, it must belong to at least one of the following subspaces and so their union:

$$\mathbf{v} \in \begin{cases} \ker(A_1 - AId) \cap \ker(A_2 - AId) \cap \ker(A_3 - DId) \\ \cup\ \ker(A_1 - AId) \cap \ker(A_2 - AId) \cap \ker(A_3) \\ \cup\ \ker(A_1 - AId) \cap \ker(A_2) \cap \ker(A_3) \\ \cup\ \ker(A_1 - AId) \cap \ker(A_2) \cap \ker(A_3 - DId) \\ \cup\ \ker(A_1) \cap \ker(A_2 - AId) \cap \ker(A_3) \\ \cup\ \ker(A_1) \cap \ker(A_2 - AId) \cap \ker(A_3 - DId) \\ \cup\ \ker(A_1) \cap \ker(A_2) \cap \ker(A_3) \\ \cup\ \ker(A_1) \cap \ker(A_2) \cap \ker(A_3 - DId) \end{cases}$$

The kernels are equal to:

$$\begin{cases} \ker(A_1 - AId) =< (1, -\frac{B}{A}, \frac{C}{A}) >=< (1, \frac{B}{\gamma+B}, -\frac{C}{\gamma+B}) > \\ \ker(A_2 - AId) =< (1, \frac{A}{B}, -\frac{C}{B}) >=< (1, -\frac{\gamma+B}{B}, -\frac{C}{B}) > \\ \ker(A_3 - DId) =< (1, -1, \frac{D}{C}) >=< (1, -1, -\frac{\gamma}{C} - \frac{C}{B}) > \\ \ker(A_1) =< (0,1,0), (0,0,1) > \\ \ker(A_2) =< (1,0,0), (0,0,1) > \\ \ker(A_3) =< (1,0,0), (0,1,0) > \end{cases}$$

Observe that:

$$\begin{aligned} \ker(A_1 - AId) \nsubseteq \ker(A_3 - DId) \quad &\implies \quad \ker(A_1 - AId) \cap \ker(A_3 - DId) = \{\vec{0}\} \\ \ker(A_2 - AId) \nsubseteq \ker(A_3 - DId) \quad &\implies \quad \ker(A_2 - AId) \cap \ker(A_3 - DId) = \{\vec{0}\} \\ \ker(A_1 - AId) \nsubseteq \ker(A_2 - AId) \quad &\implies \quad \ker(A_1 - AId) \cap \ker(A_2 - AId) = \{\vec{0}\} \end{aligned}$$

Moreover:

$$\begin{cases} \ker(A_1) \cap \ker(A_2) =< (0,0,1) > \\ \ker(A_1) \cap \ker(A_3) =< (0,1,0) > \\ \ker(A_2) \cap \ker(A_3) =< (1,0,0) > \\ \ker(A_1) \cap \ker(A_2) \cap \ker(A_3) = \{\vec{0}\} \end{cases}$$

Then, it is clear that $\mathbf{v} = \vec{0}$. In conclusion, we have proved that there does not exist 3 linearly independent generalized eigenvectors.

In other words, the system cannot be reduced into decoupled scalar DDEs. As mentioned in the Introduction, this does not imply that the system does not have any solution. Other methods with more advanced techniques have to be used. In this project, the multiple delay analysis will be performed only numerically.

2.1.2 Numerical Analysis

In this section the system in (10) will be studied throughout solutions computed through Matlab codes. Some of these codes can be found in Appendix B. The final goal is to determine the numerical stability. Numerical Stability is computed through the function *CheckStable.m*, the code of which can be also found in Appendix B.3.

Uniform delay

In the previous section, the stability of the 3-dimensional non-linear system in (10) has been studied analytically. The aim of this section is to compare the analytic and numerical stability. Furthermore, we will analyse numerically the behaviour of the linear system in (18) and compare it to the non-linear.

Firstly, we will start by the non-linear system in (10). The code for this system can be found in Appendix B.1. The figures in 8 show different solutions corresponding to each of the three stability regimes. The complete stability diagrams for the non-linear as well as the linear system with $m_u = 0.3, m_L = 0.8$ can be found in Fig. 9.

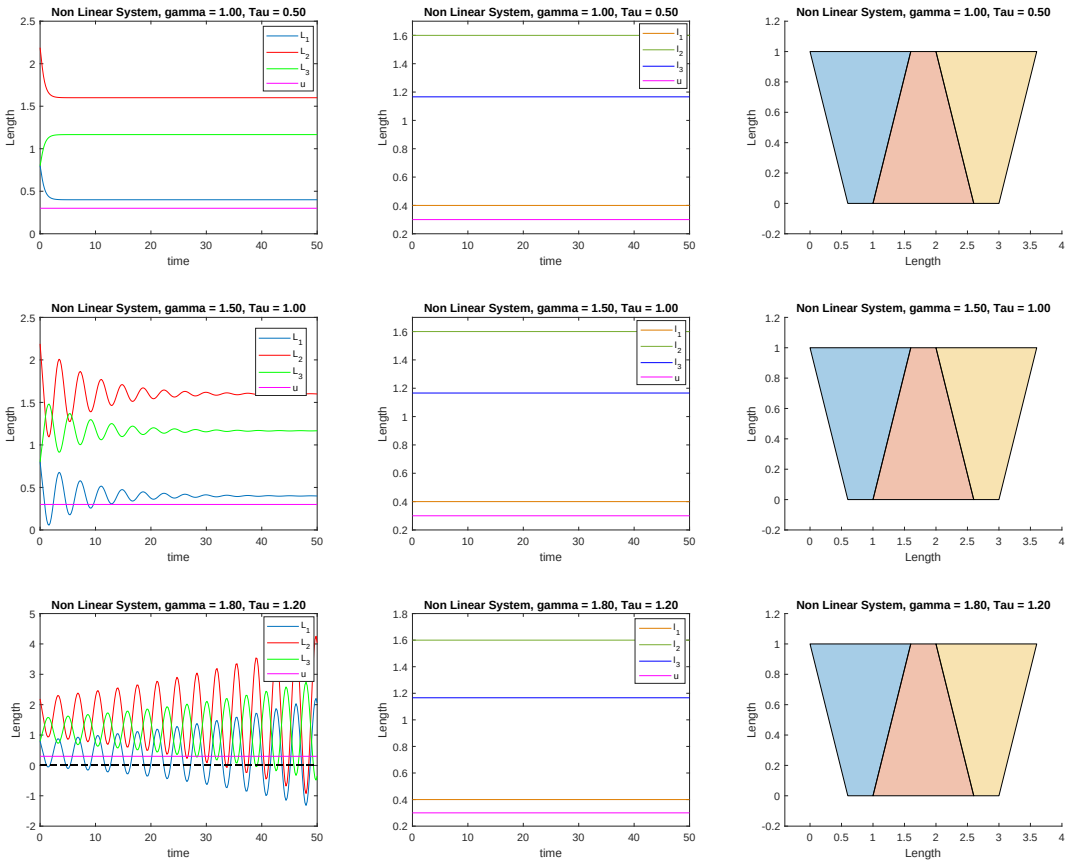

Figure 8: Solutions of the non-linear system with different stability regimes and $m_u = 0.3, m_L = 0.8$: stable non-oscillatory -superior row-, oscillatory stable -middle row- and unstable -inferior row-. Observe that for the unstable regime, the rest-length becomes negative. The reason for this will be explained in the Multiple Delay analysis.

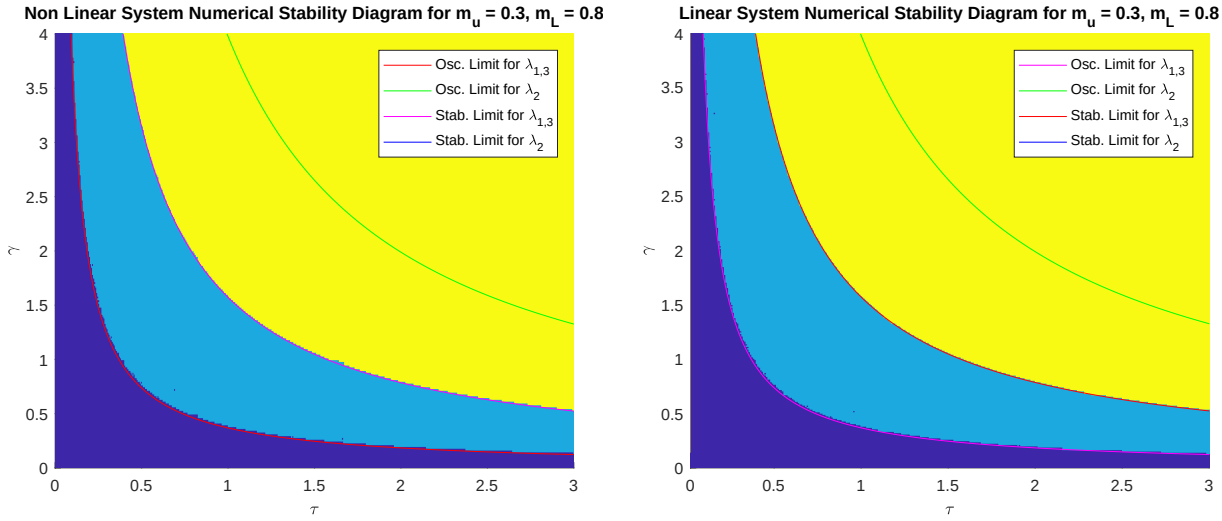

Figure 9: On the left, numerical stability of the non-linear system. On the right, numerical stability of the linear system. Stable non-oscillatory region in dark blue, oscillatory stable region in light blue and unstable region in yellow. The lines correspond to the oscillatory and stability limits found analytically. This diagram corroborates lemma 2.12.

In Fig. 9, the stability diagrams for the non-linear and the linear system can be compared. We can conclude that the results of the analytic analysis correspond to the numerical analysis. Besides, we have observed that solutions to the linear system in (18) are almost identical to the non-linear system. We suspect that the reason behind this is that $\dot{u}(t) = 0$ implies that the equilibrium condition of the non-linear system becomes linear.

Let W be elastic energy of the system defined in (3). As it was explained in the Introduction, imposing equilibrium is equivalent to the minimisation of the energy, which translates into the expression $\frac{\partial W}{\partial u} = 0$. Applying the chain rule, a new equation arises:

$$0 = \frac{\partial W}{\partial u} = \sum_i \frac{\partial W}{\partial l_i}\frac{\partial l_i}{\partial u}$$

Observe that $\dot{u} = 0$ is a solution of the non-linear system. This is not only observable numerically but can also be seen that it is a solution of the reduced version of the non-linear system deduced in (12). Due to the exclusive dependence of the deformed lengths on u, the deformed lengths are also constant. Since u and $l_i, \forall i$ are constants, we can define the constants c_i $\forall i$ and then:

$$c_i := \frac{\partial l_i}{\partial u}\,\forall i \Longrightarrow \sum_i \frac{\partial W}{\partial l_i}c_i = 0 \Longrightarrow \sum_i c_i k(l_i - L_i(t)) = 0$$

Which is a linear equilibrium equation. Notice that the other equations of the system correspond to the evolution equation of the rest-lengths described in (2), which is also linear. Therefore, the non-linear system behaves as the linear system.

Remark 2.13. This is possible thanks to the uniformity of the delay and γ. If there were different values for γ for different rest-length evolution equations or if the delay at each equation was different, this reasoning would not apply.

Multiple delays: l_i-dependant delays

It has been suggested that the delay is related to the deformed length of the cells [4]. In this section, we will study the solutions to the system in (10) with multiple delays:

$$\begin{cases} \dot{L_1}(t) = \gamma(l_0 - 2u(t-\tau_1) - L_1(t-\tau_1)) \\ \dot{L_2}(t) = \gamma(l_0 + 2u(t-\tau_2) - L_2(t-\tau_2)) \\ \dot{L_3}(t) = \gamma\left(\sqrt{l_0^2 + 4u^2(t-\tau_3)} - L_3(t-\tau_3)\right) \\ 0 = L_2(t) - L_1(t) - 6u(t) + \dfrac{2u(t)L_3(t)}{\sqrt{l_0^2 + 4u^2(t)}} \end{cases}$$

Where the delays are defined as:

$$\tau_i(t) := \alpha l_i(t-\delta) \quad \forall t, \quad i = 1, 2, 3$$

Where $\delta << 1$ is the length of the subsets in our time partition and α is the ratio at which the delay evolves. The code for this system can be found in B.2. The plots in Fig. 10 illustrate the three possible regimes of stability with $m_u = 0.3, m_L = 0.8$.

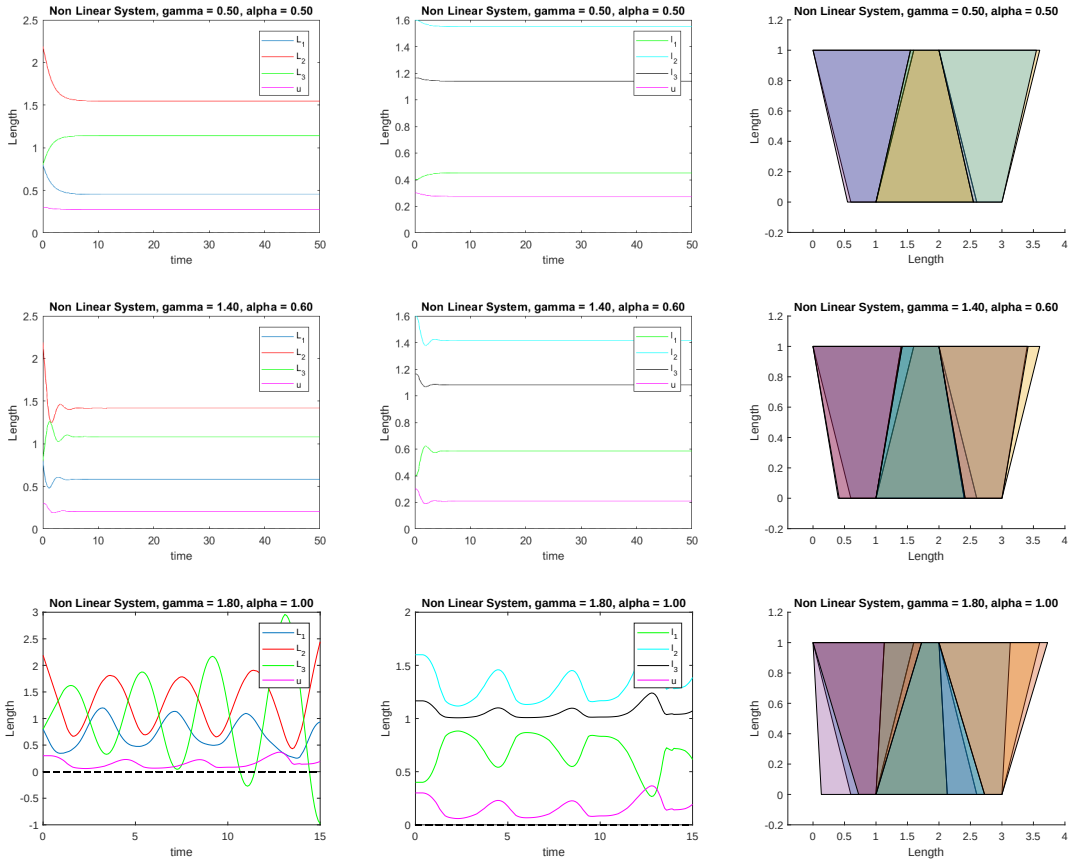

Figure 10: Stable non-oscillatory -superior row-, Oscillatory stable -middle row- and Unstable -inferior row- solutions with $m_u = 0.3, m_L = 0.8$. In the unstable case, at $t \simeq 3.5$, the rest-length becomes negative.

Observe that in contrast to the uniform delay case, the multiple delay allows oscillations in $u(t)$. The visible oscillations represented by the polygons on the right of Fig. 10 are a direct consequence of the displacement fluctuations. Furthermore, this is corroborated by the empirical observation of pulsing forces. For example, in the process of dorsal closure during *Drosophila* embryogenesis [5].

The main limitation of this model is that the rest-length or the deformed length eventually become negative. This is due to abrupt oscillations -probably caused by an unstable behaviour- and the lack of a restriction implemented in the model. In reality the appearance of a contact force is observed prior to the length becoming negative. This contact force guarantees the restriction $l \geq 0, L \geq 0$. In this project, this restriction has not been implemented, consequently, we will just consider the solutions before the length becomes negative and ignore the results after this event.

Another limitation of this method is the high sensitivity to the chosen time partition. When the deformed lengths oscillate, a not sufficiently fine partition could easily lead to the delays missing the oscillatory behaviour, which they should inherit.

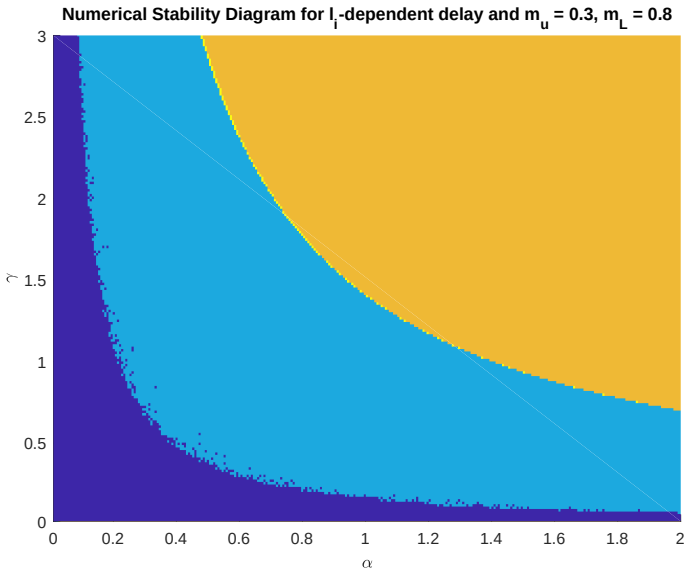

Figure 11: Stable non-oscillatory region in dark blue, oscillatory stable region in light blue. The unstable region appears in yellow, while the orange region refers to the cases where the deformed length becomes negative.

In Fig. 11, the stability diagram can be found. The orange region represents the cases where the rest-length or the deformed-length have become negative at some point. Notice the thin yellow line that separates the light blue region from the orange. This line corresponds to unstable solutions which are not affected by the limitation of our code, i.e. the lengths do not become negative.

The diagram suggests that the orange area belongs to the unstable region. Nonetheless, since our model does not consider the restrictions of positive length, we cannot ensure that all the cases belonging to the orange region are unstable.

The rest of the diagram resembles the diagrams in 9. We suspect that one of the reasons is the choice of $l_0 = 1$. However, by observing the figures in Fig. 10 it is clear that the models cannot be compared. Furthermore, the oscillatory stable region in 11 is slightly bigger than in the uniform delay case, which is intuitive since multiple delays induces different complex cell coupling mechanisms.

2.2 Second Model

Consider a strip of tissue where cells are adjacent to each other. Assume a horizontal displacement $\mathbf{u}(t)$ such that all the cells deform into the same trapezoid shape while keeping the adjacency. Let $\alpha(t)$ be the angle formed when the displacement occurs as shown in the following figure.

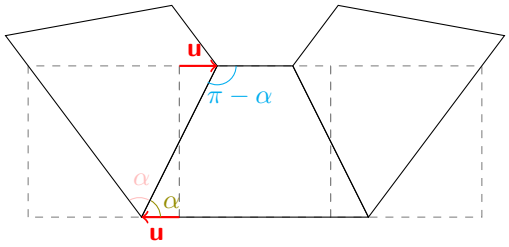

Figure 12: Effect of displacement $u(t)$ -in red- on a strip of cells in rest-position -dashed line-. The main feature of this model is that all the cells deform into the same trapezoid shape. The angle α is formed as a consequence of the displacement and it satisfies $u(t) = \frac{l_3(t)}{2} cos\ \alpha(t)$

In the first model, cells deform creating a shrinking or expanding flat area of tissue. On the contrary in this model cells fold creating curved tissue surfaces. Both models coexist and contribute to the formation of embryonic structures.

The limits of the definition intervals of $u(t)$ and $\alpha(t)$ belong to the rest-position and the limit situation which is illustrated in Fig. 13. The definition intervals are: $\alpha(t) \in [\frac{\pi}{4}, \frac{\pi}{2}]$ and $u(t) \in [0, \frac{l_0}{2}]$

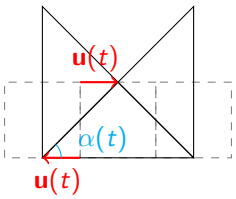

Figure 13: Limit situation occurs when $\alpha = \frac{\pi}{4}$ and $u = \frac{l_0}{2}$. When cells are in rest-position -dashed line-, $\alpha = \frac{\pi}{2}$ and $u = 0$. Observe that this limit resembles a collapsed circle.

By the reflection symmetry of the model, it suffices to focus on one side to study the stress forces acting upon the edges. Furthermore, in order to avoid an underdetermined system, mechanical equilibrium will be separately imposed at each of the superior and inferior nodes. These conditions will provide four linearly independent equations.

Let $\sigma_i(t)$ be the stress force acting upon edge i at each instant t, defined in the Introduction. Under these considerations, the force diagram can be represented as the following figure.

We proceed to impose an equilibrium condition at each node. Notice that since α is defined in $[\frac{\pi}{4}, \frac{\pi}{2}]$, then it is satisfied $sin\ \alpha, cos\ \alpha > 0$.

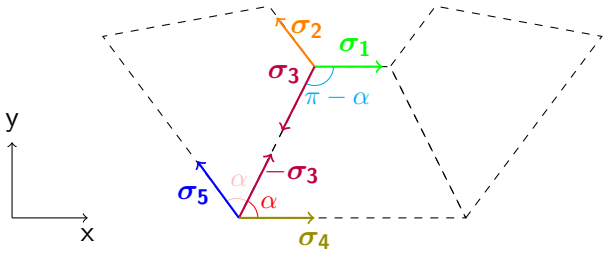

Figure 14: Stress forces acting upon the edges. The edges are labelled such that σ_i is acting on edge i.

Forces at the superior node:
The sum of the vertical components must be zero:

$$\sigma_2 sin(\pi - 2\alpha) = \sigma_3 sin\ \alpha \Rightarrow 2\sigma_2 sin\ \alpha cos\ \alpha = \sigma_3 sin\ \alpha \Rightarrow \sigma_3 = 2\sigma_2 cos\ \alpha$$

Also the sum of horizontal components must be zero:

$$\sigma_1 = \sigma_2 cos(\pi - 2\alpha) + \sigma_3 cos\ \alpha \Rightarrow \sigma_1 + \sigma_2(2cos^2\ \alpha - 1) = \sigma_3 cos\ \alpha \Rightarrow \sigma_1 = \sigma_2$$

Forces at the inferior node:
Observe that thanks to the definition of the stress force, we can use σ_3 on edge 3. Otherwise, the equilibrium condition would imply the nullity of vertical components of the forces acting upon the inferior edges and thus, a model definition problem.

The sum of the vertical forces must be zero:

$$\sigma_5 sin(\pi - 2\alpha) + \sigma_3 sin\ \alpha = 0 \Rightarrow 2\sigma_5 sin\ \alpha cos\ \alpha + \sigma_3 sin\ \alpha = 0 \Rightarrow \sigma_3 = -2\sigma_5 cos\ \alpha$$

The sum of the horizontal forces must be zero:

$$\sigma_4 - \sigma_5 cos(\pi - 2\alpha) + \sigma_3 cos\ \alpha = 0 \Rightarrow \sigma_4 + \sigma_5(2cos^2\ \alpha - 1) + \sigma_3 cos\ \alpha = 0 \Rightarrow \sigma_4 = \sigma_5$$

The equilibrium equations can be written in terms of the stress forces illustrated in Fig. 14 as well as in terms of lengths using the definition of stress force given in equation (1).

$$\begin{cases} \sigma_1 = \sigma_2 \\ \sigma_4 = \sigma_5 \\ \sigma_3 = 2\sigma_2 cos\ \alpha \\ \sigma_3 = -2\sigma_5 cos\ \alpha \end{cases} \iff \begin{cases} l_1(t) - l_2(t) = L_1(t) - L_2(t) \\ l_4(t) - l_5(t) = L_4(t) - L_5(t) \\ l_3(t) - L_3(t) = \frac{4u(t)}{l_3(t)}(l_2(t) - L_2(t)) \\ l_3(t) - L_3(t) = -\frac{4u(t)}{l_3(t)}(l_5(t) - L_5(t)) \end{cases} \tag{23}$$

Remark 2.14. A consequence of the equilibrium equations is $\sigma_2 = -\sigma_5$ and $\sigma_1 = -\sigma_4$, which is coherent with physical intuition. As it can be seen in Fig. 14, edges 4 and 5 have been expanding while edges 2 and 1 have been contracting. Besides, the contraction of edge 1 is proportional to the expansion of edge 4 and the same occurs for edges 2 and 5.

As mentioned before, the main geometrical feature of this model is that for every instant, all cells have the same shape. This property translates into geometrical conditions which we will use in order to dispose of the deformed length variables, following a parallel reasoning to the procedure for First Model.

Furthermore, from Fig. 12, it is observed that $l_1(t)$ and $l_4(t)$ directly depend on $u(t)$, in a similar way as in First Model with $l_2(t)$ and $l_1(t)$. Gathering these observations, we get four linearly independent equations.

$$\begin{cases} l_2(t) = l_1(t) \\ l_5(t) = l_4(t) \\ l_1(t) = l_0 - 2u(t) \\ l_4(t) = l_0 + 2u(t) \end{cases} \tag{24}$$

Moreover, similarly to First Model, $l_3(t)$ satisfies a geometrical condition, given the assumption of a constant cell height l_0 and the geometry illustrated in Fig. 12.

$$u^2(t) + \frac{l_0^2}{4} = \frac{l_3^2(t)}{4} \Longrightarrow l_3(t) = \sqrt{l_0^2 + 4u^2(t)} \tag{25}$$

Remark 2.15. Some equations immediately derive from these geometrical conditions: $l_1(t) + l_4(t) = 2l_0$ and $l_4(t) - l_1(t) = 4u(t)$. These equations are coherent with physical intuition, similarly to the reasoning in Remark 2.14.

Similarly to First Model, the geometrical conditions highlight the exclusive dependence of the deformed length variables on $u(t)$. This feature can be used to dispose of these variables and reduce the system. As a result, the equilibrium equations in (23) transform into the following:

$$\begin{cases} L_1(t) = L_2(t) \\ L_4(t) = L_5(t) \\ L_1(t) + L_4(t) = 2l_0 \\ 0 = l_0^2 + 12u^2(t) + 4u(t)L_1(t) - 4u(t)l_0 - \sqrt{l_0^2 + 4u^2(t)}L_3(t) \end{cases} \tag{26}$$

Lastly, every edge has a rest-length which follows the evolution equation in (2). It is again possible to apply the geometrical conditions, leading to the following DDE system.

$$\begin{cases} \dot{L_1}(t) = \gamma(l_1(t-\tau) - L_1(t-\tau)) = \gamma(l_0 - 2u(t-\tau) - L_1(t-\tau)) \\ \dot{L_2}(t) = \gamma(l_2(t-\tau) - L_2(t-\tau)) = \gamma(l_0 - 2u(t-\tau) - L_2(t-\tau)) \\ \dot{L_3}(t) = \gamma(l_3(t-\tau) - L_3(t-\tau)) = \gamma(\sqrt{l_0^2 + 4u^2(t-\tau)} - L_3(t-\tau)) \\ \dot{L_4}(t) = \gamma(l_4(t-\tau) - L_4(t-\tau)) = \gamma(l_0 + 2u(t-\tau) - L_4(t-\tau)) \\ \dot{L_5}(t) = \gamma(l_5(t-\tau) - L_5(t-\tau)) = \gamma(l_0 + 2u(t-\tau) - L_5(t-\tau)) \end{cases} \tag{27}$$

Remark 2.16. The equilibrium condition $L_1(t) = L_2(t)$ makes the first and second equations linearly dependent. The same occurs for the fourth and fifth under $L_4(t) = L_5(t)$. Besides, $L_4(t) = 2l_0 - L_1(t)$ results in the fourth equation becoming equivalent to the first.

After some transformations, only the delay differential equations for $L_1(t)$ and $L_3(t)$ remain linearly independent. This leads to the final 3-dimension non-linear system:

$$\begin{cases} \dot{L_1}(t) = \gamma(l_0 - 2u(t-\tau) - L_1(t-\tau)) \\ \dot{L_3}(t) = \gamma(\sqrt{l_0^2 + 4u^2(t-\tau)} - L_3(t-\tau)) \\ 0 = l_0^2 + 12u^2(t) + 4u(t)L_1(t) - 4u(t)l_0 - \sqrt{l_0^2 + 4u^2(t)}L_3(t) \end{cases} \tag{28}$$

This system can still be further reduced into a two equations system, disposing of $L_3(t)$. For simplicity purposes, in this development we will use the notation $z_\tau := z(t-\tau)$ and $z := z(t)$.

We can find an expression for $\dot{L_3}$ by differentiating the last equation with respect to t:

$$\dot{L_3} = \frac{(24u\dot{u} + 4\dot{u}L_1 + 4u\dot{L_1} - 4l_0\dot{u})\sqrt{l_0^2+4u^2} - (l_0^2 + 12u^2 + 4uL_1 - 4ul_0)\dfrac{4u\dot{u}}{\sqrt{l_0^2+4u^2}}}{l_0^2+4u^2}$$

By substituting the expressions for $\dot{L_3}$ and $L_{3\tau}$ in the second equation, the new expression will be written in terms of L_1 and u. We obtain the equivalent reduced 2-dimensional non-linear system:

$$\begin{cases} \dot{L_1}(t) = \gamma(l_0 - 2u_\tau - L_{1\tau}) \\ \\ \dot{u}(t) = \gamma \dfrac{4(u^3 - u_\tau^3)(2u_\tau + L_{1\tau} - 4l_0) + l_0^2(u-u_\tau)(L_{1\tau} - l_0 + 2u_\tau)}{12u^3 + 5l_0^2u + l_0^2L_1 - l_0^3} \end{cases} \tag{29}$$

This system will be used later for the numerical analysis. Nonetheless, for simplicity purposes in the analytic study we will use the system in (28).

Initial conditions

Before moving on to the analysis, we must set the initial variables to system (28). Due to the equilibrium equation, the initial situation cannot be reflected by the rest-position, but a perturbation.

We introduce two dimensionless parameters m_u and m_L, ratios of the height l_0, such that $u(0) = m_u l_0$ and $L_0 := m_L l_0$. Besides, the deformed lengths must satisfy the geometrical conditions, thus:

$$l_1(0) = l_0(1-2m_u), \qquad l_3(0) = l_0(\sqrt{1+4m_u^2}) \tag{30}$$

The perturbation of the rest state is imposed on $L_2(0)$ through the definition of a parameter $\epsilon << 1$ such that:

$$L_1(0) = L_0 = m_L l_0, \qquad L_3(0) = L_0 + \epsilon = m_L l_0 + \epsilon, \tag{31}$$

Remark 2.17. Since $L_1(0) > 0$, it is necessary $m_L > 0$. Besides, the value of m_L has a direct physical meaning: for $m_L < 1$, the cells are initially inflated, while for $m_L > 1$, the cells are initially contracted. As it was commented in First Model, we will suppose cells are initially contracted. Therefore, we will set $m_L \in [0,1]$. Also, since the deformed length is always positive, $m_u \in [-\frac{1}{2}, \frac{1}{2}]$. From this point on, this domain will be referred as D:= $[-\frac{1}{2}, \frac{1}{2}]x[0,1]$.

By imposing equilibrium, we can find an expression for ϵ:

$$\epsilon = \epsilon(l_0, m_L, m_u) = l_0\left(-m_L + \frac{1 + 12m_u^2 + 4m_u m_L - 4m_u}{\sqrt{1+4m_u^2}}\right) \tag{32}$$

Lastly, it is necessary to check if the possible values for ϵ are compatible with the positive definition of L_2. Basically, a definition problem could occur when $\epsilon < 0$. Nonetheless, as it can be seen in Fig. 15, it is positive within the domain of the parameters.

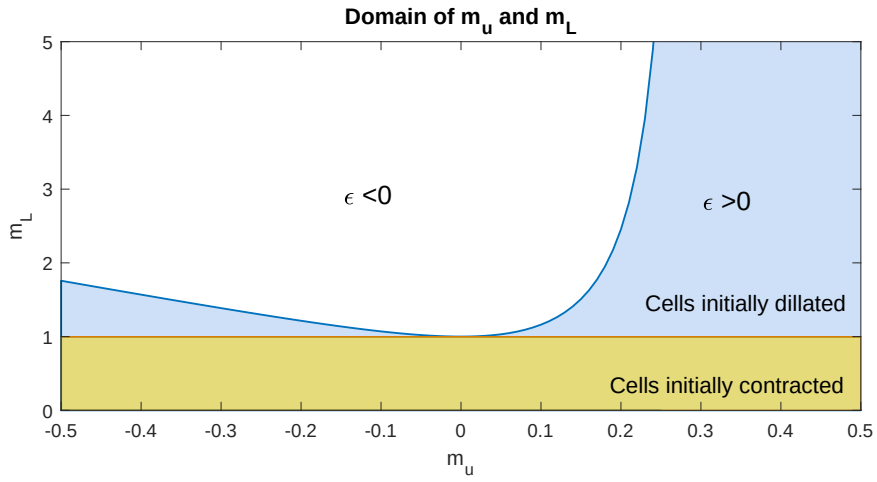

Figure 15: Curve -in blue- such that $\epsilon = 0$. Underneath, $\epsilon > 0$. In yellow, the domain for which cells are initially contracted. The area in blue and white corresponds to initially enlarged cells.

2.2.1 Linear Analysis

This analysis focuses on the non-linear system in (28), given the initial conditions in (31) and $u(0) = m_u l_0$. Due to the explanation given in the linear Analysis of First Model, we will proceed to linearise the system at the initial conditions. Once more, our final intention is to reduce the system into scalar decoupled DDEs, the stability of which has been studied in the Introduction.

By Proposition 1.14, the linearised system at the initial condition is the following. The computations can be found in A.2.

$$\begin{cases} \dot{L_1}(t) = \gamma(l_0 - 2u(t-\tau) - L_1(t-\tau)) \\ \dot{L_3}(t) = \gamma(\frac{l_0^2}{\sqrt{l_0^2+4u_0^2}} - L_3(t-\tau) + \frac{4u_0}{\sqrt{l_0^2+4u_0^2}}u(t-\tau)) \\ 4u_0\left(L_1(t) - L_{10} - 3u_0 - 6u(t) + \frac{L_{30}(u_0-u(t))}{\sqrt{l_0^2+4u_0^2}}\right) = \sqrt{l_0^2+4u_0^2}L_3(t) + (4l_0 - 4L_{10})u(t) - l_0^2 \end{cases} \tag{33}$$

Following the procedure in First Model, the next step is to isolate $u(t)$ from the last equation and find an explicit expression for $u(t-\tau)\ \ \forall t$. Nonetheless, in this case the coefficient of u may be zero and the dependency on u may be lost. More concisely, this occurs when $m_L = -12m_u^3 - 5m_u + 1$, which is the solution to the following equation and it is represented in Fig. 16.

$$-\frac{4u_0L_{30}}{\sqrt{l_0^2+4u_0^2}} - 4l_0 + 4L_{10} + 24u_0 = 0 \iff -4 + 4m_L + 24m_u - \frac{4m_u(1+12m_u^2+4m_um_L-4m_u)}{1+4m_u^2} = 0$$

Given the initial conditions on this curve, it is not possible to isolate $u(t)$ from the last equation, however it is possible to find and explicit expression for $L_3(t)$:

$$L_3(t) = \frac{4u_0^2L_{30}}{l_0^2+4u_0^2} + \frac{4u_0L_1(t) + l_0^2 - 12u_0^2 - 4u_0L_{10}}{\sqrt{l_0^2+4u_0^2}}$$

Nevertheless, the DDEs will still have dependency on $u(t-\tau)$, which makes the study of stability much more complicated. Thus, we will not study this case on this project.

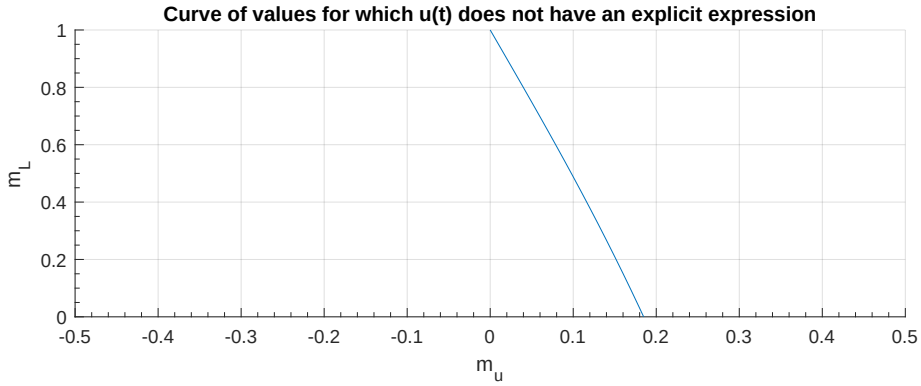

Figure 16: Curve $m_L = -12m_u^3 - 5m_u + 1$ such that $u(t)$ does not appear in the last equation.

Despite these problematic initial values, we can continue the analytic analysis for the rest of the domain D, following a similar procedure than in First Model. Thus, assume $m_L \neq -12m_u^3 - 5m_u + 1$, then $u(t)$ has an explicit expression $\forall t$:

$$u(t) = \frac{\sqrt{l_0^2+4u_0^2}L_3(t) - \left(l_0^2 - 12u_0^2 - 4u_0L_{10} + \frac{4u_0^2L_{30}}{\sqrt{l_0^2+4u_0^2}}\right) - 4u_0L_1(t)}{-\frac{4u_0L_{30}}{\sqrt{l_0^2+4u_0^2}} - 4l_0 + 4L_{10} + 24u_0} \tag{34}$$

This equation can be evaluated in $t-\tau$ in order to reduce the former system into a 2-dimensional purely-delayed linear system.

$$\begin{bmatrix}\dot{L_1}(t)\\ \dot{L_3}(t)\end{bmatrix} = \begin{bmatrix}A & B\\ C & D\end{bmatrix}\begin{bmatrix}L_1(t-\tau)\\ L_3(t-\tau)\end{bmatrix} + \gamma\begin{bmatrix} l_0 - \frac{2\left(l_0^2 - 12u_0^2 - 4u_0L_{10} + \frac{4u_0^2L_{30}}{\sqrt{l_0^2+4u_0^2}}\right)}{-\frac{4u_0L_{30}}{\sqrt{l_0^2+4u_0^2}} - 4l_0 + 4L_{10} + 24u_0} \\ \frac{l_0^2}{\sqrt{l_0^2+4u_0^2}} + \frac{4u_0\left(l_0^2 - 12u_0^2 - 4u_0L_{10} + \frac{4u_0^2L_{30}}{\sqrt{l_0^2+4u_0^2}}\right)}{\sqrt{l_0^2+4u_0^2}\left(-\frac{4u_0L_{30}}{\sqrt{l_0^2+4u_0^2}} - 4l_0 + 4L_{10} + 24u_0\right)}\end{bmatrix} \tag{35}$$

Where the matrix entries correspond to the following expressions:

$$A = -\gamma + \frac{8\gamma u_0}{-\frac{4u_0L_{30}}{\sqrt{l_0^2+4u_0^2}} - 4l_0 + 4L_{10} + 24u_0} \qquad B = \frac{-2\gamma\sqrt{l_0^2+4u_0^2}}{-\frac{4u_0L_{30}}{\sqrt{l_0^2+4u_0^2}} - 4l_0 + 4L_{10} + 24u_0}$$

$$C = \frac{-\left(\frac{16\gamma u_0^2}{\sqrt{l_0^2+4u_0^2}}\right)}{-\frac{4u_0L_{30}}{\sqrt{l_0^2+4u_0^2}} - 4l_0 + 4L_{10} + 24u_0} \qquad D = -\gamma + \frac{4\gamma u_0}{-\frac{4u_0L_{30}}{\sqrt{l_0^2+4u_0^2}} - 4l_0 + 4L_{10} + 24u_0}$$

Uniform delay

Suppose the delay represented by τ is the same for all the equations. As proceeded in First Model, we will diagonalise the system matrix in order to compute the eigenvalues, which will determine the stability of the ODE system (case $\tau = 0$), but not the delayed case. Thanks to the diagonalisation, the decoupling of the two DDEs will be possible.

Firstly, we calculate the characteristic polynomial, the roots of which correspond to the eigenvalues of the matrix:

$$0 = \begin{vmatrix} A-\lambda & B \\ C & D-\lambda \end{vmatrix} = \lambda^2 - (A+D)\lambda + AD - BC$$

Then, the eigenvalues of the system matrix are the following:

$$\lambda_1 = -\gamma, \qquad \lambda_2 = \gamma \left(\frac{-2m_u - m_L + 1}{12m_u^3 + 5m_u + m_L - 1} \right)$$

Remark 2.18. The first eigenvalue is the same as in First Model and it is real and negative. The second eigenvalue is also real but its sign depends on the initial conditions. The sign of λ_2 within the domain D is illustrated in Fig. 17. In the regions where $\lambda_2 < 0$, the system in (35) with $\tau = 0$ is non-oscillatory stable. If $\lambda_2 > 0$, the ODE system is unstable, which implies that the DDE system is also unstable, independently of the values of τ and γ.

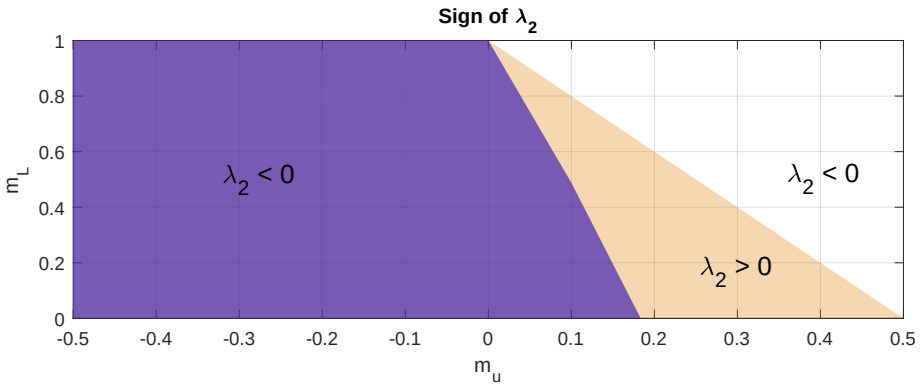

Figure 17: Regions in purple and white correspond to $\lambda_2 < 0$ -stable ODE system-. Region in orange corresponds to $\lambda_2 > 0$ -unstable ODE system-. The curve in 16 separates the purple region from the orange region and corresponds to an asymptote of λ_2.

Analytically, we can describe the regions where the sign changes $\forall (m_u, m_L) \in D$:

$$\begin{aligned} \lambda_2 > 0 \quad & \text{if } 12m_u^3 + 5m_u + m_L - 1 > 0 \text{ and } m_L < -2m_u + 1 \\ \lambda_2 = 0 \quad & \text{if } m_L = -2m_u + 1 \\ \lambda_2 < 0 \quad & \text{if } 12m_u^3 + 5m_u + m_L - 1 < 0 \text{ or } m_L > -2m_u + 1 \end{aligned}$$

The two eigenvectors correspond to the kernels of the matrices:

$$< \mathbf{v}_i >= \ker \begin{pmatrix} A-\lambda_i & B \\ C & D-\lambda_i \end{pmatrix} \Longrightarrow \qquad \mathbf{v_1} = \begin{pmatrix} 1 \\ \\ \frac{4m_u}{\sqrt{1+4m_u^2}} \end{pmatrix}, \quad \mathbf{v_2} = \begin{pmatrix} 1 \\ \\ -\frac{2m_u}{\sqrt{1+4m_u^2}} \end{pmatrix} \tag{36}$$

Remark 2.19. Notice that the eigenvectors do not depend on m_L while the eigenvalues do. The initial contraction or dilation of the cell walls will affect the intensity of the deformity but not the direction of it.

Graphically, these eigenvectors can be interpreted as:

$\mathbf{v_1}, \quad -\gamma$ $\qquad\qquad$ $\mathbf{v_2}, \quad -\lambda_2$

Figure 18: Interpretation of the eigenvectors. The red and blue arrows refer to the increase and decrease of the rest-length, respectively. Below each figure appears the related eigenvector with the associated eigenvalue.

We can interpret the eigenvectors using Fig. 18. The signs of the eigenvectors are not uniquely defined, consequently the aim of this interpretation is to determine which deformation modes -also known as eigenmodes- take place simultaneously. Observe that the factor $\sqrt{1+4m_u^2} \geq 0$. The possible deformation modes are:

(i) The first eigenmode, related to $\mathbf{v_1}$ and with associated eigenvalue $-\gamma$, corresponds to the case when both L_1 and L_3 increase/decrease simultaneously. Moreover, the pace of L_1 is greater than L_3.

(ii) The second eigenmode, related to $\mathbf{v_2}$ and with associated eigenvalue λ_2, corresponds to the case when L_1 increases while L_3 decreases, and vice versa. The pace at which L_3 decreases/increases is greater than the pace of L_1.

In contrast to the First Model, the non-delayed system is not always stable, however in order to study the stability of the DDE system, we follow a similar procedure. Let $\mathbf{M}$ be the system matrix and consider the matrix of eigenvectors $\mathbf{V}$ and the diagonal matrix of eigenvalues $\mathbf{D}$.

$$\mathbf{V} := \begin{bmatrix} 1 & 1 \\ \frac{4m_u}{\sqrt{1+4m_u^2}} & -\frac{2m_u}{\sqrt{1+4m_u^2}} \end{bmatrix} \qquad \mathbf{D} := \begin{bmatrix} -\gamma & 0 \\ 0 & \gamma\left(\frac{-2m_u-m_L+1}{12m_u^3+5m_u+m_L-1}\right) \end{bmatrix}$$

Thanks to diagonalisation, we have the decomposition $\mathbf{M} = \mathbf{V}\mathbf{D}\mathbf{V}^{-1}$. For the stability analysis we will ignore the constant term of (35). Then, the homogeneous system can be expressed as:

$$\mathbf{V}^{-1}\begin{bmatrix} \dot{L_1}(t) \\ \dot{L_2}(t) \end{bmatrix} = \mathbf{D}\mathbf{V}^{-1}\begin{bmatrix} L_1(t-\tau_1) \\ L_2(t-\tau_2) \end{bmatrix} \tag{37}$$

By defining a change of variables $\mathbf{z}(t) := \mathbf{V}^{-1}\mathbf{L}(t) \in \mathbb{R}^2$, the former system becomes two decoupled linear scalar delay differential equations:

$$\begin{bmatrix} \dot{z}_1(t) \\ \dot{z}_2(t) \end{bmatrix} = \begin{bmatrix} -\gamma & 0 \\ 0 & \gamma\left(\dfrac{-2m_u - m_L + 1}{12m_u^3 + 5m_u + m_L - 1}\right) \end{bmatrix} \begin{bmatrix} z_1(t-\tau_1) \\ z_2(t-\tau_2) \end{bmatrix} \tag{38}$$

In Proposition 1.11 the stability of this type of DDE has been studied. Following the nomenclature used in the Proposition, we define the oscillatory and stability limits for each delay differential equation:

$$\tau_{oscil}(\lambda_1) := \frac{1}{e\gamma} \qquad \tau_{oscil}(\lambda_2) := \frac{12m_u^3 + 5m_u + m_L - 1}{e\gamma\,(2m_u + m_L - 1)}$$

$$\tau_{stabil}(\lambda_1) := \frac{\pi}{2\gamma} \qquad \tau_{stabil}(\lambda_2) := \frac{\pi(12m_u^3 + 5m_u + m_L - 1)}{2\gamma\,(2m_u + m_L - 1)}$$

Remark 2.20. When $\lambda_2 > 0$ in the domain D, the oscillatory and stability limits of the second equation are both negative. This is due to the inestability of the DDE, since $\forall \tau > \tau_{stabil}(\lambda_2)$.

Proposition 1.13 states that the oscillatory and stability limits of a linear system of n decoupled DDEs are defined as:

$$\tau_{oscil} := \min(\tau_{oscil}(\lambda_1), \tau_{oscil}(\lambda_2)) \qquad \tau_{stabil} := \min(\tau_{stabil}(\lambda_1), \tau_{stabil}(\lambda_2))$$

In the case of $\lambda_2 > 0$, both limits $\tau_{oscil}, \tau_{stabil}$ are negative. By the same reasoning as in Remark 2.20, the system is unstable for all possible initial conditions within domain D.

In the case of $\lambda_2 < 0$, there exist two possibilities. For some values of m_u and m_L, the eigenvalue λ_2 could determine the oscillatory and stability limits, while for some other values, λ_1 could be the determinant of the stability. In the latter case, the stability would be equal to the stability in First Model.

In conclusion, it is necessary to determine the regions such that each eigenvalue is dominant in terms of determining the stability. Applying Proposition 1.13 on the expressions for the limits, the two cases can be written analytically:

a) The eigenvalue λ_1 determines the stability if $\dfrac{12m_u^3 + 5m_u + m_L - 1}{2m_u + m_L - 1} > 1.$

b) The eigenvalue λ_2 determines the stability if $\dfrac{12m_u^3 + 5m_u + m_L - 1}{2m_u + m_L - 1} \in (0, 1).$

Remark 2.21. As a consequence of $\lambda_2 < 0$, this quotient cannot be negative.

This differentiation based on inequalities in addition to the regions determined by sign of λ_2, gives rise to four different regions:

In Region I $:= \{m_u < 0\} \cap D$, λ_1 dominates.

In Region II $:= \{m_L > 1 - 2m_u\} \cap D$ λ_1 dominates.

In Region III $:= \{m_u > 0,\ 12m_u^3 + 5m_u + m_L - 1 < 0\} \cap D$, λ_2 dominates.

In Region IV $:= \{12m_u^3 + 5m_u + m_L - 1 > 0,\ m_L < 1 - 2m_u\} \cap D$, the system is unstable.

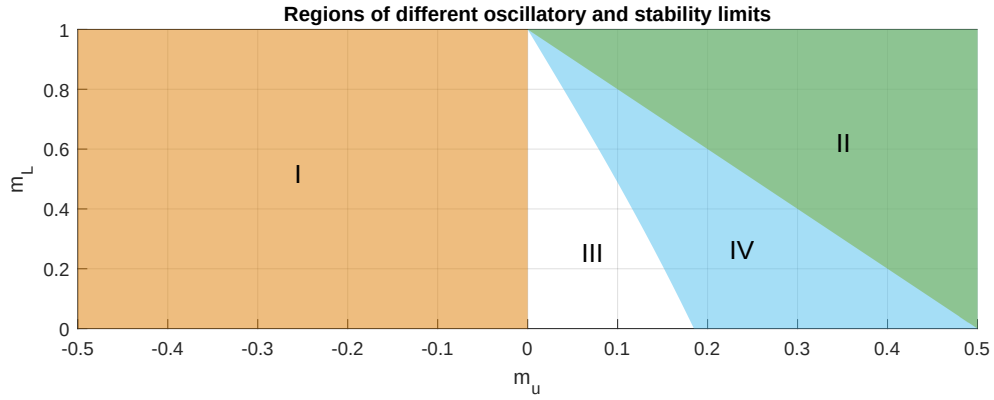

Figure 19: λ_1 dominates the stability in regions I, II. λ_2 dominates the stability in region III. In region IV, $\lambda_2 > 0$. The curve separating Regions III and IV corresponds to an asymptote in λ_2.

Conclusively, in regions I, II, the stability regime is exactly the same as in First Model. On the contrary, in region IV the system is always unstable and in region III the stability and oscillatory limits are defined by λ_2.

In Fig. 20, the limits at each region are illustrated. As it can be observed, in Regions I and II the stable non-oscillatory region is defined as the area under the blue curve, which corresponds to the oscillatory limit defined by λ_1. The oscillatory stable region is defined as the area enclosed between the blue curve and the yellow curve, which corresponds to the stability limit defined by λ_1. On the contrary, in region III, the non-oscillatory stable region is defined as the area under the orange curve, which corresponds to the oscillatory limit defined by λ_2 and the oscillatory stable region is defined as the area under the purple curve, which corresponds to the stability limit defined by λ_2. In region IV, the minimum curves are negative, therefore the system is unstable for all possible values of $\gamma > 0, \tau > 0$.

These results lead us to the formulation of the following Lemma:

Lemma 2.22. *The stability of the system in (35) not only depends on τ and γ, but also on the initial conditions m_u, m_L. Four regions with different stability regimes can be defined and each region has different expressions for the oscillatory limits and stability limits:*

In Region I, II, the stability and oscillatory limits are defined as:

$$\tau_{oscil} := \frac{1}{e\gamma} \qquad \tau_{stabil} := \frac{\pi}{2\gamma}$$

In Region III, the stability and oscillatory limits are defined as:

$$\tau_{oscil} := \frac{12m_u^3 + 5m_u + m_L - 1}{e\gamma\,(2m_u + m_L - 1)}, \qquad \tau_{stabil} := \frac{\pi(12m_u^3 + 5m_u + m_L - 1)}{2\gamma\,(2m_u + m_L - 1)}$$

In Region IV, the system is unstable for every possible value of γ, τ.

Where Regions I,II,III and IV are represented in Fig. 19 and defined above.

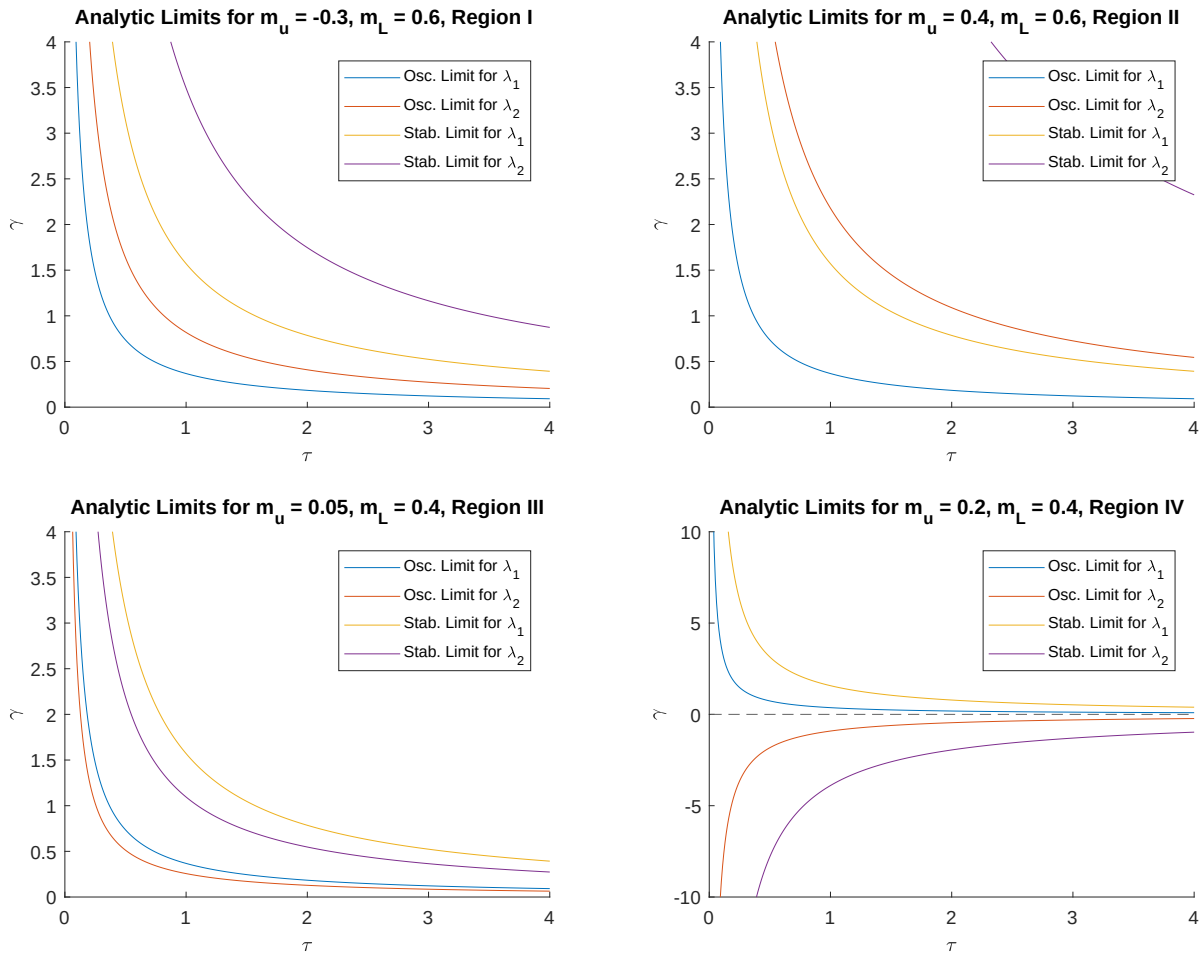

Figure 20: Analytic oscillatory and stability limits at each region. In regions I, II -top left and top right- the minimum limits are defined by λ_1. In region III -bottom left-, they are defined by λ_2. In region IV -bottom right-, the minimum limits are negative and the system is unstable.

2.2.2 Numerical Analysis

In this section the system in (28) will be studied throughout solutions computed through Matlab codes. The codes are very similar to the ones for First Model, therefore they are not included. The final goal is to determine the numerical stability of this system. Numerical Stability is computed through the function *CheckStable.m*, the code of which can be found in Appendix B.3.

Uniform delay

We will start by the non-linear system in (28). Consider a unique delay for all the equations. The figures in 21 exemplify how the solutions behave under the three stability regimes with $m_u = 0.3, m_L = 0.8$.

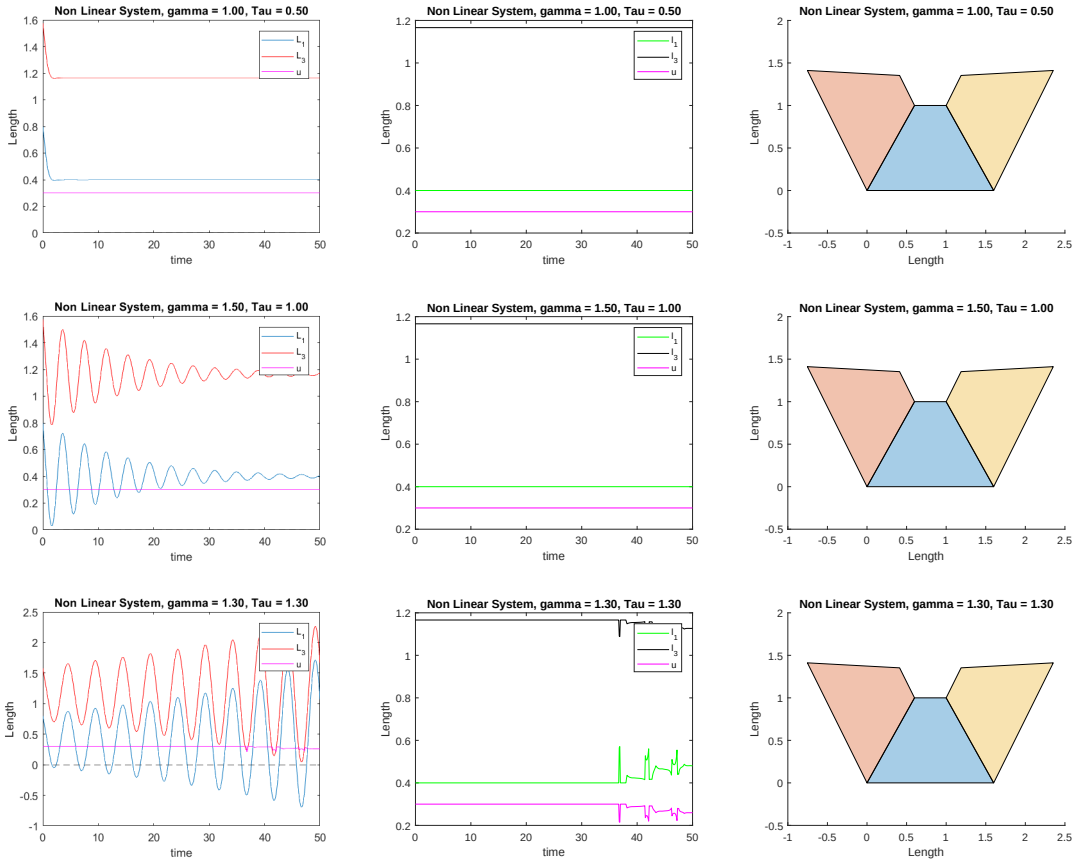

Figure 21: Stable non-oscillatory -superior row-, Oscillatory stable -middle row- and unstable -inferior row- results with $m_u = 0.3, m_L = 0.8$. Observe that for the unstable regime, the rest-length becomes negative.

When the lengths become negative, the model loses the physical interpretation. As commented in the numerical analysis of the First Model, this occurs because the restriction that ensures positive lengths is not implemented in our model. Because of this, we can say that our model does not reflect reality when the lengths become negative and therefore in such cases the results are not reliable.

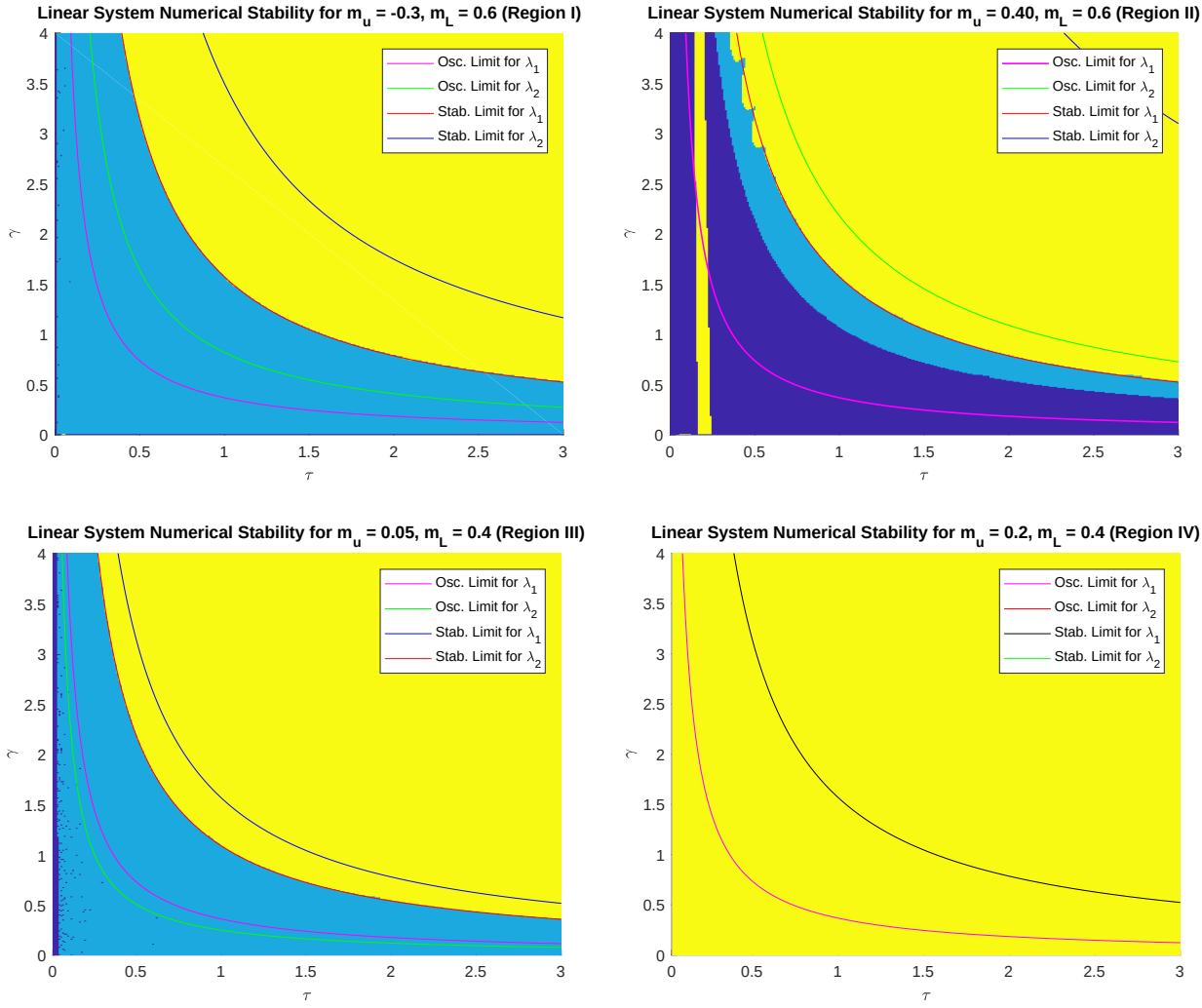

Figure 22: Stability Diagrams for the linear system in regions I and II -on top- and regions III and IV -on bottom-.

The stability diagrams in Fig. 22 show the complexity that supposes corroborating the analytic results when the stability depends on initial conditions and different regions with different regimes appear. Besides, the fact that regions III and IV are separated by an asymptote of λ_2 may affect the diagrams. Lastly, the limitations of the function *CheckStable* may also arise. Nevertheless, some points are concordant with Lemma 2.22: the instability of Region IV is finally corroborated by the numerical result as bottom right plot in Fig. 22 shows. Moreover, the unstable boundary in Regions I and III also fits the numerical stability boundary as it can be seen in the diagrams at left top and bottom.

With respect to Regions I and III, the stable non-oscillatory boundaries in both cases seem vague and we cannot corroborate the analytic oscillatory limits. We suspect the reason behind this is that the function *CheckStable* is not detecting properly the oscillatory behaviour in these cases. For instance, top left and top right plots from Fig. 23 are detected as oscillatory stable and they could be considered non-oscillatory. Therefore, we conclude that in this case the numerical results do not contradict the analytic.

With respect to Region II, despite the wavy shape for small delays, the instability boundary seems to fit the stability limit given by λ_1. Moreover, we suspect that the yellow strip that appears in the top right diagram in Fig. 22 is due to the fact that our model does not have any restriction to guarantee the positive sign of the lengths. For instance, bottom left and middle plots in Fig. 23 are detected as unstable but since the length becomes negative, the result is not reliable.

Lastly, regarding the oscillatory behaviour boundary in Region II, the cases above the magenta curve which are detected as non-oscillatory are also affected by the lack of a restriction to guarantee the positive sign of the lengths. For instance, bottom right plot in Fig. 23 is detected as non-oscillatory but since the length becomes negative, we cannot tell its behaviour apart.

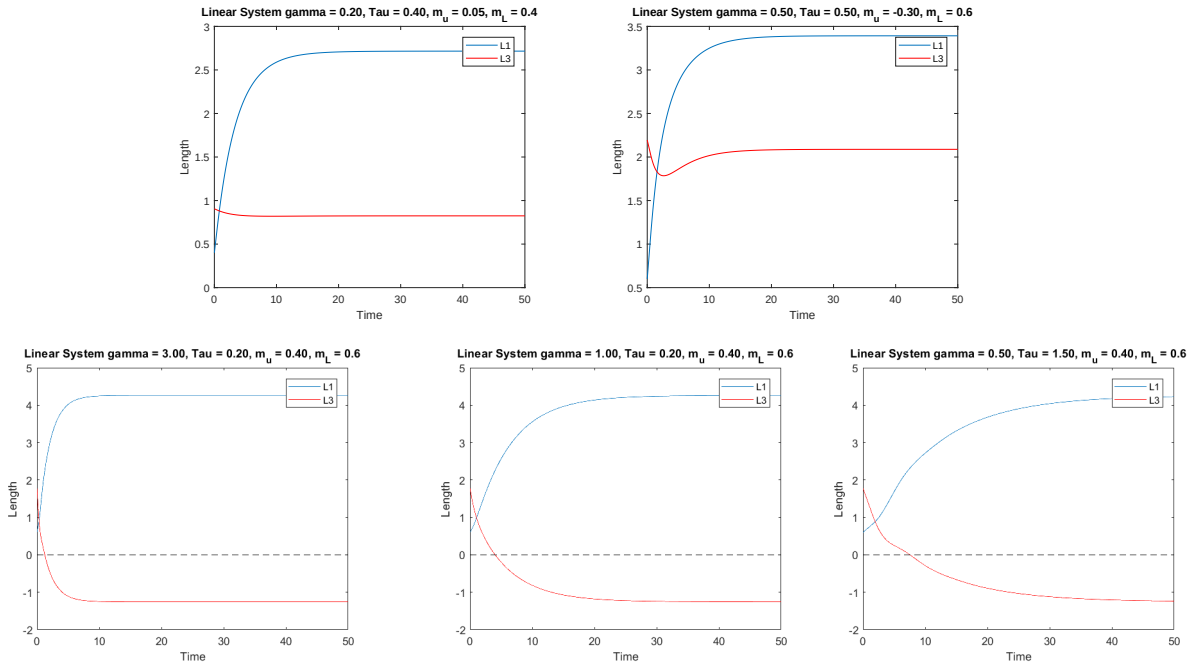

Figure 23: Examples of problematic cases where the numerical stability does not coincide with the analytic.

In conclusion, we cannot affirm that the numerical results confirm Lemma 2.22. However, we have studied the conflicting cases and discussed that they may be misleading due to the limitations of our model and the method of computing the numerical stability. Therefore, we can say that the numerical results do not contradict the analytical results.

Multiple delays: l_i dependant delay

It has been suggested that the delay is related to the deformed length of the cells [4]. In this section, we will study the solutions to the non-linear system in (28) with multiple delays defined as follows:

$$\begin{cases} \dot{L_1}(t) = \gamma(l_0 - 2u(t-\tau_1) - L_1(t-\tau_1)) \\ \dot{L_3}(t) = \gamma(\sqrt{l_0^2 + 4u^2(t-\tau_3)} - L_3(t-\tau_3)) \\ 0 = l_0^2 + 12u^2(t) + 4u(t)L_1(t) - 4u(t)l_0 - \sqrt{l_0^2 + 4u^2(t)}L_3(t) \end{cases}$$

Where the delays are defined as:

$$\tau_i(t) = \alpha l_i(t-\delta) \quad \forall t, \quad i = 1, 3$$

Where $\delta << 1$ is the length of the subsets in our time partition and α is the ratio at which the delay evolves.

The plots in Fig. 25 illustrate the three possible regimes of stability with $m_u = 0.3, m_L = 0.8$. The limitations of this method are the same as commented in section 2.1.2. As mentioned in the First Model, the multiple delay allows oscillations in $u(t)$. The visible oscillations represented by the polygons on the right of Fig. 25 are a direct consequence of the displacement oscillations.

In Fig. 24 the stability diagram can be found. Compared to the First Model diagram in Fig. 11, the non-oscillatory stable region has enlarged and the thin yellow line representing the unstable cases not affected by the limitations of our model has vanished. This suggests that the boundary of the stable region in the stability diagram cannot be told apart, in contrast with First Model.

Apart from the highlighted differences, the analysis leads to very similar conclusions to section 2.1.2.

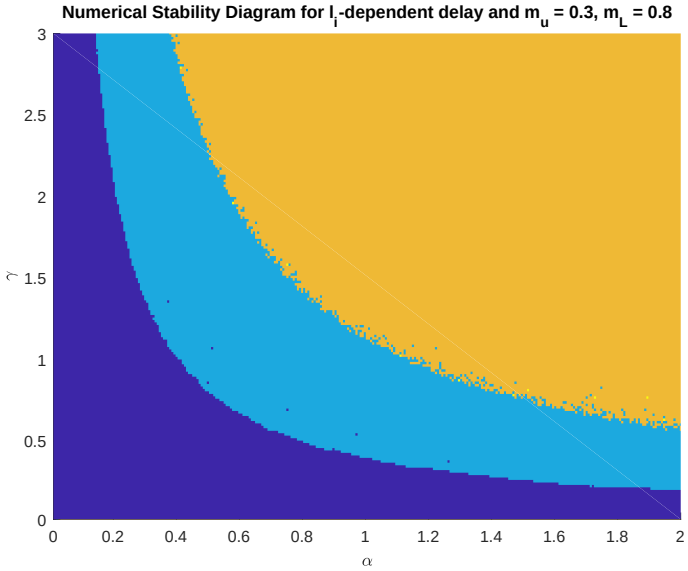

Figure 24: Stable non-oscillatory region in dark blue, oscillatory stable region in light blue. The unstable region appears in yellow, while the orange region refers to the cases where the deformed length becomes negative.

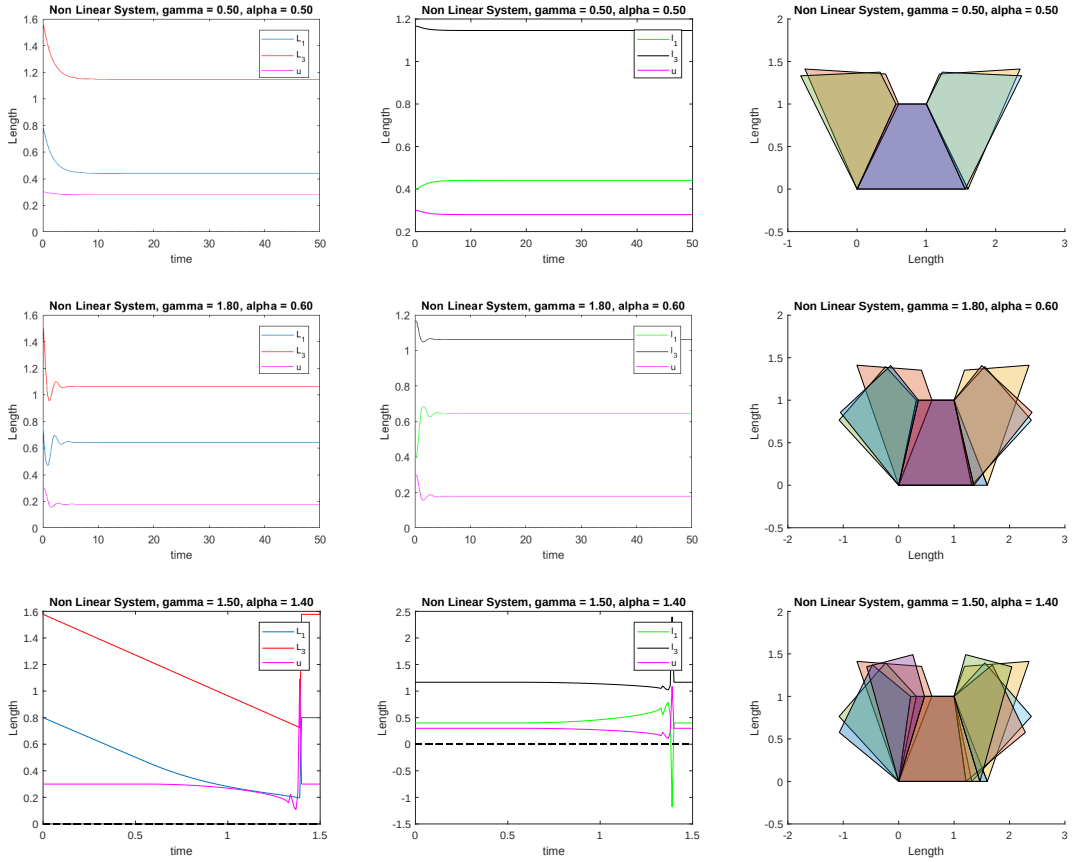

Figure 25: Stable non-oscillatory -superior row-, Oscillatory stable -middle row- and Unstable -inferior row- results with $m_u = 0.3, m_L = 0.8$. The polygons in the right plot correspond to different selected instants. In the unstable case, the deformed length becomes negative, making the solution no longer reliable.

3. Conclusions

In the First Model under the uniform delay hypothesis, the limits of the oscillatory and stability behaviour found in the analytic analysis in Lemma 2.12 have been corroborated by the numerical analysis. In Fig. 9 we can appreciate the precision with which the analytic stability and oscillatory limits fit the numerical stability boundaries. Besides, the linear behaviour of the non-linear system has been proved for solutions with constant displacement. These two facts lead us to the final confirmation of Lemma 2.12 applied to the non-linear system, i.e. the explicit expressions for the stability boundaries of the non-linear system in terms of τ and γ.

For the First Model under the multiple delay hypothesis, in the analytic study we have proved that the system cannot be expressed as decoupled scalar delay differential equations. Numerically the limitations of our model of l_i-dependent delays appear remarkable, since as it can be seen in Fig. 11 the vast majority of unstable cases may be affected by the limitations of our model. We have also discussed the resemblance with the stability diagrams of the uniform delay case and stated that this resemblance is not conclusive, due to the magnitude order chosen for the deformed length. Besides, a more accurate model is required in order to properly establish the real numerical stability boundaries.

In the Second Model, the analytic analysis was only performed with uniform delay and it shows that the stability boundaries are dependent on initial conditions. The definition of four regions within the considered initial conditions domain is required to classify the stability of the system. In one of the regions, the system is always unstable. In two other regions, the stability of the system is exactly the same as First Model. In the remaining region, the stability boundaries are defined by other expressions determined by the second eigenvalue. These results are gathered in Lemma 2.22.

In contrast with the First Model, the numerical results for the uniform delay case acquired in Fig. 22 do not corroborate the analytic results. Nonetheless, the instability of Region III has been confirmed and the analytic stability limits coincide with the numerical stability boundaries in all the cases except Region II, where small differences appear. We suspect that these differences are due to the numerical limitations of our method to detect stability. Furthermore, the oscillatory behaviour does not appear to coincide with the regions described in the analytic study. The controversial cases have been discussed with the conclusion that they may be due to numerical limitations.

The multiple delay case of the Second Model has only been studied numerically. The behaviour resembles the multiple delay case of the First Model, nevertheless the stable non-oscillatory region is larger in the Second Model. Furthermore, the thin yellow line representing the unstable cases and showing the boundary of the oscillatory stable region does not appear in the Second Model. This suggests that the oscillatory stable area might be larger than the corresponding region shown in the diagram 24. However, the results are not conclusive.

3.1 Future Work

One of the initial assumptions we made in the Introduction was to assume a constant cell height. This assumption certainly is a simplification of reality. It has been observed in mammalian embryogenesis that the internal pressure is a mechanism of size control and changes in pressure and size can affect cell allocation and fate [6]. Then, it is clear that fluctuations in height also exist and our models cannot appreciate these effects. Consider the Second Model without the assumption of constant height and assume an internal pressure. The internal pressure generates a normal force pushing the walls outwards. Figure 26 shows how pressure affects the cell walls. The corresponding force diagram can be found in Fig. 27.

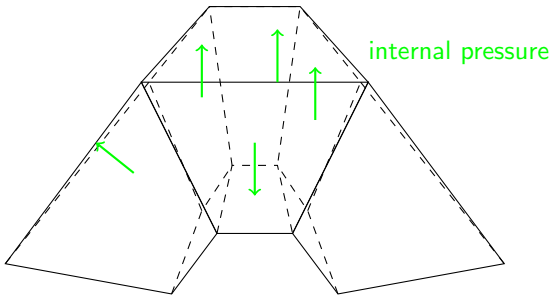

Figure 26: The internal pressure acts on the cell walls perpendicularly.

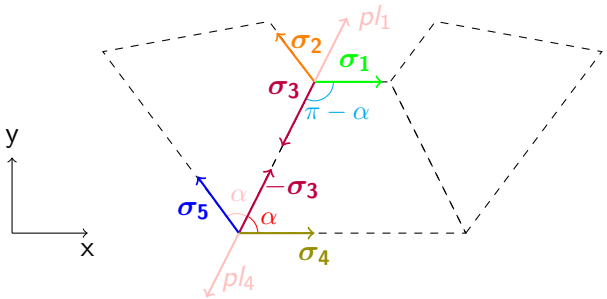

Figure 27: Stress forces acting upon the edges. The edges are labelled such that σ_i is acting on edge i. The internal pressure is represented by p.

The choice of a convenient equilibrium condition -such that the resulting equations are solvable- becomes more complicated and it requires further study. Our expectations are that the work developed for the Second Model creates a basis for this study.

Another piece of future work is the analytic study of the multiple delay systems, which requires a more advanced knowledge of delay differential equations. Thus it would be possible to create a better numerical model for the length-dependent delays, such that the restrictions of positive length are taken into account in addition to the corresponding contact force activation. Moreover, the results of such improved model could be compared with the numerical results acquired in this project to determine the influence of this restriction in the global behaviour of the system.

Lastly, we would like to study further the stability of the Second Model and improve our method to detect the numerical stability in order to clarify the numerical results obtained in this project.

4. Bibliography

References

[1] T. Erneux. *Applied delay differential equations*, Surveys and tutorials in the applied mathematical sciences Volume 3, Springer, 2009.

[2] J.J. Muñoz, M. Dingle, M. Wenzel. *Mechanical oscillations in biological tissues as a result of delayed rest-length changes*, Physical review E, 26 November 2018, vol. 98, num. 5.

[3] Sun Yi, A. G. Ulsoy. *Solution of a System of Linear Delay Differential Equations Using the Matrix Lambert Function*, 2006 American Control Conference, Minneapolis, MN, 2006, 0743-1619.

[4] A. Sumi, P. Hayes, A. D'Angelo, J. Colombelli, G. Salbreux, K. Dierkes, J. Solon. *Adherens Junction Length during Tissue Contraction Is Controlled by the Mechanosensitive Activity of Actomyosin and Junctional Recycling*, Dev. cell 47(4):453-463, 2018.

[5] J. Solon, A. Kaya-Copur, D. Brunner. *Pulsed Forces Timed by a Ratchet-like Mechanism Drive Directed Tissue Movement during Dorsal Closure*. Cell, 58(137):1331-1342, 2009.

[6] Chii Jou Chan, M. Costanzo, T. Ruiz-Herrero, G. Mnke, R.J. Petrie, M. Bergert, A. Diz-Muñoz, L. Mahadevan, T. Hiiragi. *Hydraulic control of mammalian embryo size and cell fate*, Nature (2019).

[7] A. Brugus, E. Anon, V. Conte, J.H. Veldhuis, M. Gupta, J. Colombelli, J.J. Muñoz, G. W. Brodland, B. Ladoux, X. Trepat. *Forces driving epithelial wound healing*, Nature physics **10**, 683-690 (2014).

A. Developments and Computations

A.1 First Model Linearisation

Here you can find the development to deduce system (16). In order to study the stability of the system, we will linearise it at the initial condition. Actually, since the first two equations are already linear, only the last two will be affected. Let $\mathbf{f}$ be defined as:

$$\begin{bmatrix} \dot{L_1}(t) \\ \dot{L_2}(t) \\ \dot{L_3}(t) \\ 0 \end{bmatrix} = \mathbf{f} \begin{pmatrix} L_1 \\ L_2 \\ L_3 \\ u \end{pmatrix} = \begin{bmatrix} \gamma(l_0 - 2u(t-\tau) - L_1(t-\tau)) \\ \gamma(l_0 + 2u(t-\tau) - L_2(t-\tau)) \\ \gamma\left(\sqrt{l_0^2 + 4u^2(t-\tau)} - L_3(t-\tau)\right) \\ L_2(t) - L_1(t) - 6u(t) + \dfrac{2u(t)L_3(t)}{\sqrt{l_0^2 + 4u^2(t)}} \end{bmatrix}$$

The linearisation of $\mathbf{f}$ is defined as:

$$\mathbf{f} \begin{pmatrix} L_1 \\ L_2 \\ L_3 \\ u \end{pmatrix} \simeq \mathbf{f} \begin{pmatrix} L_0 \\ L_0 + \epsilon \\ L_0 \\ u_0 \end{pmatrix} + \mathbf{Df} \begin{pmatrix} L_0 \\ L_0 + \epsilon \\ L_0 \\ u_0 \end{pmatrix} \begin{bmatrix} L_1 - L_0 \\ L_2 - L_0 - \epsilon \\ L_3 - L_0 \\ u - u_0 \end{bmatrix}$$

Where:

$$\mathbf{Df} \begin{pmatrix} L_0 \\ L_0 + \epsilon \\ L_0 \\ u_0 \end{pmatrix} = \begin{bmatrix} -\gamma & 0 & 0 & -2\gamma \\ 0 & -\gamma & 0 & +2\gamma \\ 0 & 0 & -\gamma & \frac{4\gamma u_0}{\sqrt{l_0^2+4u_0^2}} \\ -1 & +1 & +\frac{2u_0}{\sqrt{l_0^2+4u_0^2}} & -\frac{\epsilon}{u_0} - \frac{8u_0^2 L_0}{\left(l_0^2+4u_0^2\right)^{\frac{3}{2}}} \end{bmatrix} = \begin{bmatrix} -\gamma & 0 & 0 & -2\gamma \\ 0 & -\gamma & 0 & +2\gamma \\ 0 & 0 & -\gamma & \frac{4\gamma m_u}{\sqrt{1+4m_u^2}} \\ -1 & +1 & +\frac{2m_u}{\sqrt{1+4m_u^2}} & -6 + \frac{2m_L}{(1+4m_u^2)^{\frac{3}{2}}} \end{bmatrix}$$

and

$$\mathbf{f} \begin{pmatrix} L_0 \\ L_0 + \epsilon \\ L_0 \\ u_0 \end{pmatrix} = \begin{bmatrix} \gamma l_0 - \gamma 2u_0 - \gamma L_0 \\ \gamma l_0 + \gamma 2u_0 - \gamma L_0 \\ \gamma\sqrt{l_0^2 + 4u_0^2} - \gamma L_0 \\ 0 \end{bmatrix} = \begin{bmatrix} \gamma l_0(1 - 2m_u - m_L) \\ \gamma l_0(1 + 2m_u - m_L) - \gamma\epsilon \\ \gamma l_0(\sqrt{1 + 4m_u^2} - m_L) \\ 0 \end{bmatrix}$$

$$\mathbf{Df}\begin{pmatrix} L_0 \\ L_0+\epsilon \\ L_0 \\ u_0 \end{pmatrix}\begin{bmatrix} L_1-L_0 \\ L_2-L_0-\epsilon \\ L_3-L_0 \\ u-u_0 \end{bmatrix} = \begin{bmatrix} \gamma(L_0+2u_0-2u-L_1) \\ \gamma(L_0+\epsilon-2u_0+2u-L_2) \\ \gamma(L_0-\frac{4u_0^2}{\sqrt{l_0^2+4u_0^2}}+\frac{4u_0}{\sqrt{l_0^2+4u_0^2}}u-L_3) \\ -\frac{2u_0L_0l_0^2}{(l_0^2+4u_0^2)^{\frac{3}{2}}}-L_1+L_2+\frac{2u_0}{\sqrt{l_0^2+4u_0^2}}L_3+\left(-\frac{\epsilon}{u_0}-\frac{8u_0^2L_0}{(l_0^2+4u_0^2)^{\frac{3}{2}}}\right)u \end{bmatrix} =$$

$$= \begin{bmatrix} \gamma(l_0(m_L+2m_u)-2u-L_1) \\ \gamma(\epsilon+l_0(m_L-2m_u)+2u-L_2) \\ \gamma\left(l_0\left(m_L-\frac{4m_u^2}{\sqrt{1+4m_u^2}}\right)+\frac{4m_u}{\sqrt{1+4m_u^2}}u-L_3\right) \\ -\frac{2m_um_Ll_0}{(1+4m_u^2)^{\frac{3}{2}}}-L_1+L_2+\frac{2m_u}{\sqrt{1+4m_u^2}}L_3+\left(-6+\frac{2m_L}{(1+4m_u^2)^{\frac{3}{2}}}\right)u \end{bmatrix}$$

Leading to:

$$\mathbf{f}\begin{pmatrix} L_1 \\ L_2 \\ L_3 \\ u \end{pmatrix} \simeq \begin{bmatrix} -\gamma & 0 & 0 & -2\gamma \\ 0 & -\gamma & 0 & +2\gamma \\ 0 & 0 & -\gamma & \frac{4\gamma m_u}{\sqrt{1+4m_u^2}} \\ -1 & +1 & +\frac{2m_u}{\sqrt{1+4m_u^2}} & -6+\frac{2m_L}{(1+4m_u^2)^{\frac{3}{2}}} \end{bmatrix}\begin{bmatrix} L_1 \\ L_2 \\ L_3 \\ u \end{bmatrix} + \begin{bmatrix} \gamma l_0 \\ \gamma l_0 \\ \frac{\gamma l_0}{\sqrt{1+4m_u^2}} \\ -\frac{2m_Lm_ul_0}{(1+4m_u^2)^{\frac{3}{2}}} \end{bmatrix}$$

By Proposition 1.14, we can define the linearised system as the following:

$$\begin{cases} \dot{L_1}(t) = \gamma(l_0-2u(t-\tau)-L_1(t-\tau)) \\ \dot{L_2}(t) = \gamma(l_0+2u(t-\tau)-L_2(t-\tau)) \\ \dot{L_3}(t) = \gamma\left(\frac{l_0}{\sqrt{1+4m_u^2}}+\frac{4m_u}{\sqrt{1+4m_u^2}}u(t-\tau)-L_3(t-\tau)\right) \\ 0 = -\frac{2m_Lm_ul_0}{(1+4m_u^2)^{\frac{3}{2}}}-L_1(t)+L_2(t)+\frac{2m_u}{\sqrt{1+4m_u^2}}L_3(t)+\left(-6+\frac{2m_L}{(1+4m_u^2)^{\frac{3}{2}}}\right)u(t) \end{cases}$$

A.2 Second Model Linearisation

Here you can find the development to deduce system (35). In order to study the stability of the system, we will linearise it at the initial condition. For simplicity purposes, we will use the three equations system to linearise:

$$\begin{cases} \dot{L_1}(t) = \gamma(l_0 - 2u(t-\tau) - L_1(t-\tau)) \\ \dot{L_3}(t) = \gamma(\sqrt{l_0^2 + 4u^2(t-\tau)} - L_3(t-\tau)) \\ 0 = l_0^2 + 12u^2(t) + 4u(t)L_1(t) - 4u(t)l_0 - L_3(t)\sqrt{l_0^2 + 4u^2(t)} \end{cases}$$

The linearisation of $\mathbf{f}$ is defined as:

$$\mathbf{f}\begin{pmatrix} L_1 \\ L_3 \\ u \end{pmatrix} \simeq \mathbf{f}\begin{pmatrix} L_{10} \\ L_{30} \\ u_0 \end{pmatrix} + \mathbf{Df}\begin{pmatrix} L_{10} \\ L_{30} \\ u_0 \end{pmatrix}\begin{bmatrix} L_1 - L_{10} \\ L_3 - L_{30} \\ u - u_0 \end{bmatrix}$$

$$\mathbf{Df} = \begin{bmatrix} -\gamma & 0 & -2\gamma \\ 0 & -\gamma & \gamma\dfrac{4u_\tau}{\sqrt{l_0^2 + 4u_\tau^2}} \\ 4u & -\sqrt{l_0^2 + 4u^2} & 24u + 4L_1 - 4l_0 - \dfrac{4u}{\sqrt{l_0^2 + 4u^2}}L_3 \end{bmatrix}$$

$$\begin{bmatrix} \dot{L_1} \\ \dot{L_3} \\ 0 \end{bmatrix} \simeq \begin{bmatrix} -\gamma & 0 & -2\gamma \\ 0 & -\gamma & \frac{4u_0\gamma}{\sqrt{l_0^2+4u_0^2}} \\ 4u_0 & -\sqrt{l_0^2 + 4u_0^2} & -\frac{4u_0L_{30}}{\sqrt{l_0^2+4u_0^2}} - 4l_0 + 4L_{10} + 24u_0 \end{bmatrix}\begin{bmatrix} L_1 \\ L_3 \\ u \end{bmatrix} + \begin{bmatrix} \gamma l_0 \\ \gamma\frac{l_0^2}{\sqrt{l_0^2+4u_0^2}} \\ l_0^2 - 12u_0^2 - 4L_{10}u_0 + \frac{4u_0^2L_{30}}{\sqrt{l_0^2+4u_0^2}} \end{bmatrix}$$

By Proposition 1.14, we can define the linearised system as the following:

$$\begin{cases} \dot{L_1}(t) = \gamma(l_0 - 2u(t-\tau) - L_1(t-\tau)) \\ \dot{L_3}(t) = \gamma(\frac{l_0^2}{\sqrt{l_0^2+4u_0^2}} - L_3(t-\tau) + \frac{4u_0}{\sqrt{l_0^2+4u_0^2}}u(t-\tau)) \\ 4u_0\left(L_1(t) - L_{10} - 3u_0 - 6u(t) + \frac{L_{30}(u_0-u(t))}{\sqrt{l_0^2+4u_0^2}}\right) = \sqrt{l_0^2 + 4u_0^2}L_3(t) + (4l_0 - 4L_{10})u(t) - l_0^2 \end{cases}$$

B. Codes

Here you can find three of the codes that were used for this project. We did not add the rest because they are very similar to these. All of them refer to the First Model.

B.1 Non Linear System First Model

The following code solves the system in (10).

```
gamma = 1.8; Tau = 1.2; mL = 0.8; mu = 0.3;
%Partition settings
delta_t = 0.2; tmax = 50; numTimePoints = floor(tmax/delta_t);
multTau = floor(Tau/delta_t); %Aproximation of Tau as a multiple of delta_t
%Initial settings
l0 = 1; L0 = mL*l0; u0 = mu*l0; epsilon = 2*l0*mu*(3 - (mL/sqrt(1 + 4*(mu^2))));
L10 = L0; L20 = L0 + epsilon; L30 = L0;
L1 = L10*ones(numTimePoints,1); L2 = L20*ones(numTimePoints,1);
L3 = L30*ones(numTimePoints,1); u = u0*ones(numTimePoints,1);

if (multTau == 0)
    %Newton on many variables
    for i = 2:numTimePoints
        x_prev = [L1(i-1); L2(i-1); L3(i-1); u(i-1)];
        x = x_prev;
        j = 0; rel_error = 1; convergence = 0;
        while (not(convergence) && j<10)
           m = sqrt((l0^2) + (4*(x(4)^2)));
           f = [((x_prev(1)-x(1))/delta_t)+(gamma*(l0-2*x(4)-x(1)));
               ((x_prev(2)-x(2))/delta_t)+(gamma*(l0+2*x(4)-x(2)));
               ((x_prev(3)-x(3))/delta_t)+(gamma*(m-x(3)));
               x(2)-x(1)-(6*x(4))+(2*x(4)*x(3)/m)];
           Df = [-gamma-(1/delta_t),0,0,-2*gamma;
               0,-gamma-(1/delta_t),0,+2*gamma;
               0,0,-gamma-(1/delta_t),gamma*4*x(4)/m;
               -1,+1,+2*x(4)/m,-6-(8*(x(4)^2)*x(3)/(m^3))+(2*x(3)/m)];
           xj = x - (Df\f);
           rel_error = norm(xj - x) / norm(xj);
           convergence = rel_error < 1.e-10;
           j = j+1; x = xj;
        end
        L1(i) = x(1); L2(i) = x(2); L3(i) = x(3); u(i) = x(4);
    end
else
    for i = 2:numTimePoints
        x_prev = [L1(i-1); L2(i-1); L3(i-1); u(i-1)];
        if (multTau >= i)
```

```
            x_del = [L10;L20;L30;u0]; %column of size(4,1)
        else
            x_del = [L1(i-multTau); L2(i-multTau); L3(i-multTau); u(i-multTau)];
        end
        x = x_prev;
        x(1) = x_prev(1)+(delta_t*gamma*(l0-2*x_del(4)-x_del(1)));
        x(2) = x_prev(2)+(delta_t*gamma*(l0+2*x_del(4)-x_del(2)));
        x(3) = x_prev(3)+(delta_t*gamma*(sqrt(l0^2+4*(x_del(4)^2))-x_del(3)));
        L1(i) = x(1); L2(i) = x(2); L3(i) = x(3);
        %Newton 1D on the equilibrium equation
        y = x_prev(4);
        j = 0; rel_error = 1; convergence = 0;
        while (not(convergence) && j<10)
           m = sqrt((l0^2)+(4*(y^2)));
           f = x(2)-x(1)-(6*y)+(2*y*x(3)/m);
           Df = -6-(8*(y^2)*x(3)/(m^3))+(2*x(3)/m);
           yj = y - (f/Df);
           rel_error = norm(yj - y) / norm(yj);
           convergence = rel_error < 1.e-10;
           j = j+1; y = yj;
        end
        u(i) = y;
    end
end
S = max([CheckStable(L1),CheckStable(L2),CheckStable(L3)]);
```

B.2 Non Linear System First Model with l_i- dependant delays

The following code solves the system described in section 2.1.2.

```
%Partition settings
delta_t = 0.1; tmax = 50; numTimePoints = floor(tmax/delta_t);
%Initialisation of variables
gamma = 1.8; alpha = 1; mL = 0.8; mu = 0.3; l0 = 1; L0 = mL*l0; u0 = mu*l0;
epsilon = 2*l0*mu*(3 - (mL/sqrt(1 + 4*(mu^2)))); L10 = L0; L20 = L0 + epsilon;
L30 = L0; l10 = l0 - 2*u0; l20 = l0 + 2*u0; l30 = l0*sqrt(1 + 4*(mu^2));
L1 = L10*ones(numTimePoints,1); L2 = L20*ones(numTimePoints,1);
L3 = L30*ones(numTimePoints,1); u = u0*ones(numTimePoints,1);
l1 = l10*ones(numTimePoints,1); l2 = l20*ones(numTimePoints,1);
l3 = l30*ones(numTimePoints,1);

for i = 2:numTimePoints
    if (l1(i-1)<0 || l2(i-1)<0 || l3(i-1)<0) %the delay is not well defined
        break;
    elseif (alpha == 0)
    %Newton on many variables
```

```
    x_prev = [L1(i-1); L2(i-1); L3(i-1); u(i-1)]; x = x_prev;
    j = 0; rel_error = 1; convergence = 0;
    while (not(convergence) && j<10)
       m = sqrt((l0^2) + (4*(x(4)^2)));
       f = [((x_prev(1)-x(1))/delta_t)+(gamma*(l0-2*x(4)-x(1)));
           ((x_prev(2)-x(2))/delta_t)+(gamma*(l0+2*x(4)-x(2)));
           ((x_prev(3)-x(3))/delta_t)+(gamma*(m-x(3)));
           x(2)-x(1)-(6*x(4))+(2*x(4)*x(3)/m)];
       Df = [-gamma-(1/delta_t),0,0,-2*gamma;
           0,-gamma-(1/delta_t),0,+2*gamma;
           0,0,-gamma-(1/delta_t),gamma*4*x(4)/m;
           -1,+1,+2*x(4)/m,-6-(8*(x(4)^2)*x(3)/(m^3))+(2*x(3)/m)];
       xj = x - (Df\f);
       rel_error = norm(xj - x) / norm(xj); convergence = rel_error < 1.e-10;
       j = j+1; x = xj;
    end
    L1(i) = x(1); L2(i) = x(2); L3(i) = x(3); u(i) = x(4);
else
    Tau1 = alpha*l1(i-1); multTau1 = floor(Tau1/delta_t);
    Tau2 = alpha*l2(i-1); multTau2 = floor(Tau2/delta_t);
    Tau3 = alpha*l3(i-1); multTau3 = floor(Tau3/delta_t);
    x_prev = [L1(i-1); L2(i-1); L3(i-1); u(i-1)]; x = x_prev;
    if (multTau1 >= i)
        x_del(1) = L10; u1 = u0;
    else
        x_del(1) = L1(i-multTau1); u1 = u(i-multTau1);
    end
    if (multTau2 >= i)
        x_del(2) = L20; u2 = u0;
    else
        x_del(2) = L2(i-multTau2);  u2 = u(i-multTau2);
    end
    if (multTau3 >= i)
        x_del(3) = L30; u3 = u0;
    else
        x_del(3) = L3(i-multTau3); u3 = u(i-multTau3);
    end
    x(1) = x_prev(1)+(delta_t*gamma*(l0-2*u1-x_del(1)));
    x(2) = x_prev(2)+(delta_t*gamma*(l0+2*u2-x_del(2)));
    x(3) = x_prev(3)+(delta_t*gamma*(sqrt(l0^2+4*(u3^2))-x_del(3)));
    L1(i) = x(1); L2(i) = x(2); L3(i) = x(3);
    y = x_prev(4);
    j = 0; rel_error = 1; convergence = 0;
    while (not(convergence) && j<10)
       m = sqrt((l0^2)+(4*(y^2)));
       f = x(2)-x(1)-(6*y)+(2*y*x(3)/m);
```

```
            Df = -6-(8*(y^2)*x(3)/(m^3))+(2*x(3)/m);
            yj = y - (f/Df);
            rel_error = norm(yj - y) / norm(yj); convergence = rel_error < 1.e-10;
            j = j+1; y = yj;
        end
        u(i) = y; l1(i) = l0 - 2*u(i); l2(i) = l0 + 2*u(i); l3(i) = sqrt((l0^2) + (4*(u(i)^2))
    end
end
S = max([CheckStable(L1),CheckStable(L2),CheckStable(L3)]);
```

B.3 CheckStable

This function, provided by my supervisor Jose Javier Muñoz, classifies the stability of a function. It returns an integer S, such that when $S = -1$ the function is non-oscillatory stable, when $S = 1$ it is oscillatory stable and when $S = 4$, unstable. This function was used to paint the numerical stability diagrams.

```
function [S,l]=CheckStable(L)
    n=length(L); Max=zeros(n,1); Min=zeros(n,1); k=1; km=1;
    Sunst=4; SstabOsc=1; SstabNOsc=-1;
    tol=1e-3; % tolerance for relative value
    tolL=1e-10;
    if norm(L(floor(95*n/100):n))<eps
        S=Sunst; % Unstable if analysis could not finish
    else
        for i=3:n
            if L(i)+tolL<L(i-1) && L(i-1)>L(i-2)+tolL % One local maximum detected
                Max(k)=i-1;
                k=k+1;
            end
        end
        for i=3:n
            if L(i)>L(i-1)+tolL && L(i-1)+tolL<L(i-2) % One local minimum detected
                Min(km)=i-1;
                km=km+1;
            end
        end
        Lerr=abs(L(end)-L(end-1))/abs(mean(L));
        if k==1 && km==1 %There is NO oscillation (no maxima, no minima detected)
            if Lerr>tol  || isnan(L(end)) || isinf(L(end))
                S=Sunst; %Unestable Non-oscillatory
            else
                S=SstabNOsc; % Stable Non-oscillatory
            end
            l=0;
        elseif k>2 && km>2
            if L(Max(k-1))>L(Max(k-2)) && L(Min(km-1))<L(Min(km-2))
```

```
                S=Sunst; % OScillatory unstable
                l=Max(k-1)-Max(k-2);
            elseif L(Max(k-1))<=L(Max(k-2)) && L(Min(km-1))>=L(Min(km-2))
                S=SstabOsc; %Oscillatory stable
                l=Max(k-1)-Max(k-2);
            elseif Lerr >tol
                S=Sunst;
                l=0;
            else
                S=SstabOsc;
                l=0;
            end
        elseif k==2
            if Lerr>tol
                S=Sunst;
                l=0;
            else
                S=SstabOsc;
                l=0;
            end
        elseif km==2
            if Lerr>tol
                S=Sunst;
                l=0;
            else
                S=SstabOsc;
                if k>2
                    l=Max(k-1)-Max(k-2);
                else
                    l=0;
                end
            end
        else
            if Lerr>tol
                S=Sunst;
                l=0;
            else
                S=SstabNOsc;
            end
        end
    end
end
```